UNIVERSIDADE DE LISBOA
FACULDADE DE CIÊNCIAS
DEPARTAMENTO DE ENGENHARIA GEOGRÁFICA, GEOFÍSICA E ENERGIA

Selection of Paste and Glue Elements for CPV Modules

Sebastião Manuel de Lacerda Coelho

Mestrado em Engenharia da Energia e do Ambiente

2010

UNIVERSIDADE DE LISBOA
FACULDADE DE CIÊNCIAS
DEPARTAMENTO DE ENGENHARIA GEOGRÁFICA, GEOFÍSICA E ENERGIA

Selection of Paste and Glue Elements for CPV Modules

Sebastião Manuel de Lacerda Coelho

Dissertação de Mestrado em Engenharia da Energia e do Ambiente

Trabalho realizado sob a supervisão de:

Doutor Miguel Centeno Brito (FCUL)

Doutor Gianfranco Sorasio (WS Energia)

2010

Aknowledgments

I would like to thank Miguel Brito for all the support and given teaching during development of this thesis.

To Gianfranco Sorasio I would like to thank the integration opportunity in WS Energia for the development of the present thesis and also the advices and guidance during the development of this work.

I would like to thank to WS Energia team, especially to Filipa Reis, Luís Pina, Mendes Lopes and João Wemans, for the guidance and great opportunity in HSUN project integration.

I would like to thank my family members and my friends, especially to Ana Galhetas, André Brás and Flávio Figueira for all the supporting and encouraging me to pursue this degree. Without this encouragement, I would not have finished the degree.

Abstract

This thesis reports on the progress of the development of encapsulation methods and materials to use in the HSUN PV receiver. The HSUN is a concentration photovoltaic (CPV) system concept under development by WS Energia. After a thorough description of the encapsulation state of the art, two main approaches were tested: Ethylene Vinyl Acetate (EVA) laminates and Silicone stacks.

Experimental results were unsatisfactory regarding the EVA laminates. The curing process was not fully optimized which lead to (i) the appearance of yellowness after exposing the laminate to concentrated irradiation for a few days; and (ii) the increase of the series resistance of the solar cell during the curing process, probably associated to stretching of the soldered contacts. Numerical thermal modelling of the EVA laminate has also shown the need to introduce active cooling of the PV receiver in order to prevent thermal damage to the cell.

The silicone stacks tests were satisfactory regarding the optical, mechanical and electrical properties of the PV receiver. Even after a few days of concentrated irradiation there was no evidence of the development of yellowness or moisture. Thermal modelling showed that further optimization of the HSUN receiver concept is required but suggest that passive cooling approaches are probably sufficient to warrant safe thermal conditions for the solar cell even under concentrated irradiation.

Key-words: CPV; Encapsulation; EVA; Silicone; Cooling.

Resumo

O desenvolvimento da presente tese é baseado na pesquisa de materiais e desenvolvimento de métodos de encapsulamento. Tem como principal objectivo, uma aplicação no projecto HSUN, que visa o desenvolvimento de um módulo fotovoltaico de concentração (CPV) na WS Energia.

Após uma descrição pormenorizada do estado de arte do encapsulamento, foram testadas duas abordagens: Laminação de amostras com Acetato de Etileno Vinil (EVA) e Silicone.

Os resultados experimentais podem ser considerados satisfatórios atendendo à qualidade dos laminados de EVA. O processo de cura não estava completamente optimizado o que poderá ter conduzido a (i) aparecimento de amarelamento após exposição das amostras à luz concentrada durante alguns dias; e (ii) o aumento das resistências de série da célula durante o processo de cura. Este facto poderá ser associado ao alongamento dos contactos soldados. A modelação do modelo térmico para o laminado de EVA também demonstrou a necessidade de introdução de um arrefecimento activo no módulo PV de modo a evitar que a temperatura provoque danos nas células.

As amostras de silicone revelaram resultados satisfatórios em relação às propriedades ópticas, mecânicas e eléctricas do módulo PV. Após exposição da amostra à concentração solar durante alguns dias, não foi evidenciando o aparecimento de amarelamento ou humidade. O modelo térmico revelou que é necessária uma optimização do conceito HSUN. As aproximações efectuadas sugerem que um modelo de arrefecimento passivo será suficiente para garantir as condições óptimas para a célula quando submetida à irradiação concentrada.

Palavras-chave: CPV; Encapsulamento; EVA; Silicone; Arrefecimento

Abbreviations

Al	Aluminium
a-Si	Amorphous silicon
BP	British Petroleum
CdTe	Cadmium Telluride
CIGS	Cooper Indium Gallium Selenide
CPV	Concentrating Photovoltaics
C.R.	Chemical Reaction
c-Si	Single Crystal Silicone
DC	Direct Current
ENC	Encapsulant
EVA	Ethylene Vinyl Acetate
FC	Fast Cure
FCUL	Faculdade de Ciências da Universidade de Lisboa
FF	Fill Factor
GaInP	Galium Indium Phosphide
GaInAs	Galium Indium Arsenide
Ge	Germanium
IEC	International Electrotechnical Commission
IR	Infrared
I_{SC}	Short-Circuit Current
ISE	Institute for Solar Energy
JPL	Jet Propulsion Laboratories
MD	Machine Direction
MJ	Multijunction
m-Si	Multi Crystal Silicone
PET	Polyethylene Terephtlate
PE	Polyethylene

PDMS	Polydimethylsiloxane
PV	Photovoltaic
PVB	Polyvinyl Butyral
PVF	Polyvinyl fluoride
PVDF	Polyvinylidene fluoride
TD	Tensile Direction
THV	Tetrafluoroethylene Hexafluoropropylene Vinylidene fluoride
TPU	Thermoplastic Urethane
Rconv	Convective Resistance
Rcool	Cooling Resistance
R&D	Research and Development
RH	Relative Humidity
R_S	Series Resistance
R_{SH}	Shunt Resistance
RTI	Relative Thermal Index
UFC	Ultra Fast Cure
UV	Ultraviolet
V_{OC}	Open Circuit Voltage
WVTR	Water Vapor Transmission Rate
YI	Yellowness Index

Índex

Figure Index

Table Index

1. Introduction

1.1 Context of the thesis

This master thesis has been developed in the framework of a collaboration between the research and development (R&D) department of WS Energia and the *Departamento de Engenharia Geográfica Geofísica e Energia from Faculdade de Ciências da Universidade de Lisboa* (FCUL) on the development of a new photovoltaic concentrator, namely HSUN.

The HSUN is a high efficiency concentrating photovoltaic (CPV) system based on reflective optics. The design concentration level is 15 suns [Lopes, 2010]. The PV receiver accommodates silicon solar cells specifically designed for use in CPV which have to be encapsulated to protect the cells from outdoor exposure for the lifetime of the system. The focus of this thesis is precisely the development of the encapsulating materials and methods for the HSUN PV receiver [WS Energia, 2010].

1.2 Scope and objectives of the thesis

The main aim that has motivated the current thesis is to provide a detailed discussion of the materials, methods, and encapsulating alternatives for the HSUN PV receiver. This discussion includes the analysis of the module reliability and the consequences that can result in the choice of the encapsulating material.

The objectives of this thesis are as follow:

1- Review of the existing encapsulating materials and methods for the PV industry;

2- Test and characterization of two different encapsulating processes and different materials involved in the lamination process;

3- Heat transfer model for a preliminary identification of the HSUN concentrator cooling requirements.

1.3 Structure of the thesis

The current thesis is organized in two parts 7 chapters.

Chapter 1 describes the context and identifies the scope and objectives for making an efficient analysis of all the encapsulating materials for concentration.

Chapter 2 presents an overview of state of art in concentrating photovoltaic technologies.

Chapter 3 summarizes the state of art of encapsulant methods and materials for photovolaics. A lamination description is performed and the main materials for conventional modules described. A comparison between two specific encapsulants, EVA and silicones is executed.

Chapter 4 contains the description of the experimental tests performed during the development of this thesis. A pre-adhesion test, followed by procedure to encapsulate solar cells with the two encapsulants that ends with a comparison between *I-V* curves to evaluate the effect of the encapsulant in the electrical cell parameters.

Chapter 5 presents a development of a heat transfer model of the PV receiver for the HSUN and the identification of the cooling requirements for a more effective passive cooling.

Chapter 6 and 7 presents the main conclusions of this work, as well as suggestions for future developments, including the integration in the HSUN project.

2. Fundamentals of CPV Technology

This section describes the fundamental concepts of Concentrated Photovoltaic (CPV) systems and the main reasons for the increasing interest in this technology.

2.1 Overview of CPV

CPV system has recently gained interest based on its scalability and expected low levelized cost of electricity [Swanson, 2000; Luque *et al.*, 2006].

The CPV potential reduction in system costs vary widely according to the type of cells, concentration ratio, type of optics (refractive or reflective) [Luque and Hegedus, 2003] and geometry. In any case, it is important to take into account that the reduction of costs achieved with concentrators, due to the reduction of cell area, should be balanced against increased costs associated to the additional optics, tracking system and the loss of diffuse light [Reis *et al.*, 2009].

The design of a CPV system should consider the following primary parameters:

i. **Performance** - Optical efficiency, cell cooling, and performance losses associated with manufacturing imperfections, soiling, tracking errors, flexing in the wind, thermal expansion/contraction, or wind stow.

ii. **Cost** - Use of inexpensive components, ease/automation of assembly

iii. **Reliability** - Degradation of optics, poor performance of tracker or other loss of alignment, loss of adhesion or breakdown of bonds between cell and the optics and heat sink, etc.

2.2 CPV Technologies

Over the last 20 years concentrator systems have been using either reflecting or refracting cheap optical elements in order to concentrate light onto the solar cells.

CPV technologies are usually classified into three main categories: low, medium and high concentration systems, (Table 2.1) [Tripanagnostopoulos *et al*, 2005; Luque and Andreev, 2007]. The higher the concentration level, the less solar cell material is required but the higher are the requirements on the optics, alignment, etc.

Middle scaled concentrator power plants present a great potential because it does not require a tracking system as precise as the high concentration. Swanson (2003) gives a detailed overview of the concentrator activities all over the world.

Table 2.1 - Description of CPV classes according with the concentration [adapted from Kurtz, 2009].

Class of CPV	Typical Concentration Ratio	Type of Converter
Enhanced concentration modules	<3X	Silicon modules
Medium-concentration, cells	~3X-100X	Silicon or other cells
High Concentration, MJ cells	>100X	Multijunction

Low concentration CPV systems typically use conventional modules, with one or more flat mirrors. A highlight technology is the 2-suns concentrator Double-Sun™ from WS-Energia, a V-through concentration system that integrates a 2-axes tracking system which increases the amount of radiation falling onto the modules by using two flat mirrors (Figure 2.1).

(a) **(b)**

Figure 2.1- Double-Sun™ concentrator: a) DoubleSun™ photograph from a solar park in Italy; b) DoubleSun™ concentrator [WS Energia, 2010].

One advantage of the medium concentrating when compared to high concentration is that the tracking requirements are not so demanding and are therefore less expensive. When compared to low concentration, the need for silicon solar cells is reduced and therefore there may be a commercial advantage in a demand driven market. The HSUN target is to be placed inside medium concentrators range.

An example of medium concentration is the EUCLIDES™ concentrator system using parabolic mirrors that reach a geometrical concentration from 2suns up to 50suns. The EUCLIDES™ concentrator plant (Figure 2.2) in the south of Tenerife is a project of different solar research groups. It is one of the largest parabolic mirror concentrator power plant used worldwide [Sala *et al.*, 1999].

(a) **(b)**

Figure 2.2 - Concentrating system using parabolic mirrors: a) Parabolic mirror reflecting the incoming sunlight onto a focus line; b) EUCLIDES ™ concentrator plant in Tenerife [Morilla *et al.*, 2006].

Entech concentrator (20 suns) uses domed Fresnel lens to focus the light into a row of modified silicon cells, with larger contacts to reduce series resistance Joule losses. A prismatic dielectric element covers the cells and acts as secondary optics that directs the light to the active cell area [PVMaT, 2010].

CPower concentrators, Rondine Generation 1 and 2 (25 and 20 suns, respectively), uses glass to protect cells and aluminium in the back module [Antonini *et al.*, 2009]. Another concentrator prototype in this range is Traxle 5suns, that uses a bifacial flat panel, as shown in Figure 2.3 [Poulek *et al.*, 2008].

(a) **(b)**

Figure 2.3 - Parabolic concentrators: a) Rondine Gen1 with 25 suns; b) Bifacial 5X concentrator at CULS, Praha [CPower, 2010 ; Poulek et al., 2008].

The different types of high concentration systems (C > 100X) share the common feature of having 3D-based optics, multijunction (MJ) cells and use 2-axis trackers. Additionally, these systems require some sort of active cooling that can occupy a significant part and cost of the system.

The Solar Systems™ in Australia and the SunPower™ in the USA are developing two-axes tracked reflective dish concentrators and water-cooled close packed PV arrays for use in the focus (Figure 2.4) [SolarSystems, 2010]. The parabolic reflective dishes have a geometrical concentration of approximately 340 suns. The encapsulating system is usually liquid, placed by injection between the Fresnel lens and the optics.

(a) **(b)**

Figure 2.4 - High concentrator systems: a) Dish concentrator concept (The light is reflected by a parabolic dish mirror to a PV array at the focus); b) Dish concentrator system of the company Solar Systems™ in Australia [SolarSystems, 2010].

Concentrator systems with refractive optical elements work either with point (Figure 2.5) or linear Fresnel lenses (Figure 2.6).

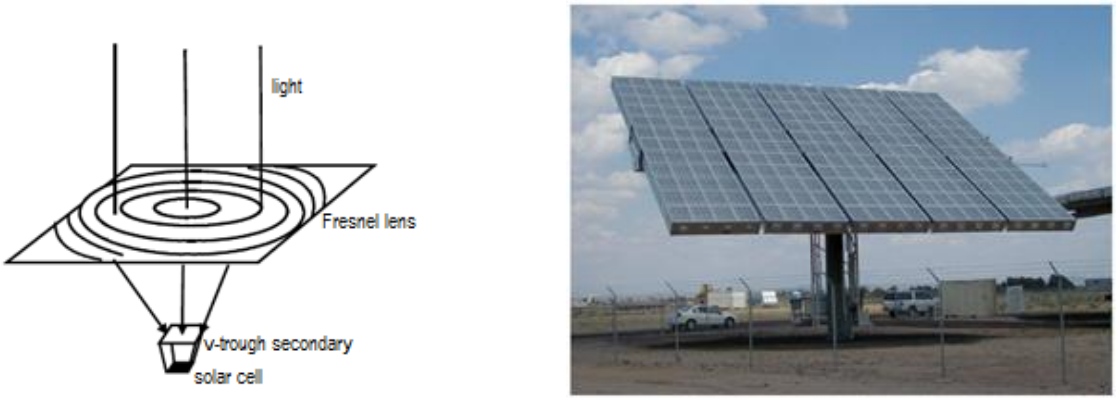

(a) (b)

Figure 2.5 - Concentrator systems with refractive optical elements a) The incoming light is concentrated by using Fresnel lenses. b) Five Mega Modules of Amonix™ assembled on a 20 kWp generation system [Amonix, 2010].

(a) (b)

Figure 2.6 – Concentrator systems with refractive optical elements a) Linear Fresnel lens concentrator concept. b) Entech™ 100 kW PV power plant [Spinoff, 2002].

Two-axes tracked point-Fresnel lens arrays are being developed by Amonix™ in the USA where 500 suns have been reached. This system uses secondary optical elements called V-trough secondaries in the centre of the lens in order to increase the acceptance.

Figure 2.7 summarizes the different typical optical approaches to CPV [Miller *et al.*, 2009].

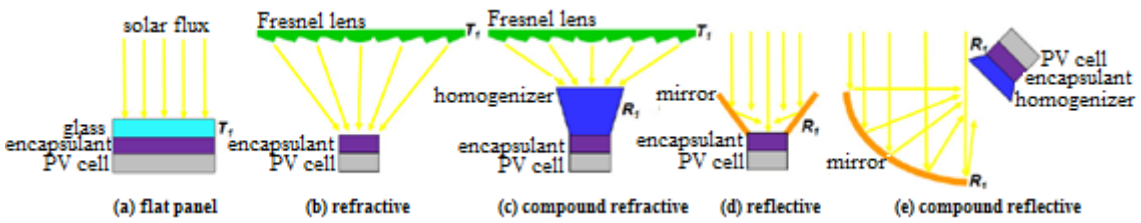

Figure 2.7 - Cross-sectional schematic identifying optical components present in: (a) conventional FP-PV, (b) & (c) refractive CPV, and (d) & (e) reflective CPV systems [Miller *et al.,* 2009].

2.3 Overview of solar cells for CPV

In the last 10 years, CPV system has witnessed a fast evolution of device technology from the wafer based silicon cells to composite photovoltaic systems Swanson (2000) and Hering (2007).

The PV market has long been dominated by single-junction solar cells based on silicon wafers including single crystal (c-Si) and multi-crystalline silicone (m-Si). Figure 2.8, illustrates a common p-n junction cell made on a silicon wafer. As shown, the n-type layer is thinner, and it is negatively doped with phosphorus. The p-type layer is larger and is positively doped with boron. When the two layers are brought together and exposed to sunlight, an electric field is created in the p-n junction, thus creating a separation between electrons and holes generated by the radiation. With an external load attached to the two layers via metal contacts, a DC current is created. Several new technologies including BP solar [Bruton *et al.*, 2003], Sanyo [Sanyo, 2010] and Sun Power [Sun Power, 2010] are increasing the commercial single-crystal wafer silicon solar cells' efficiencies to the 15–21% range, as shown in Figure 2.9.

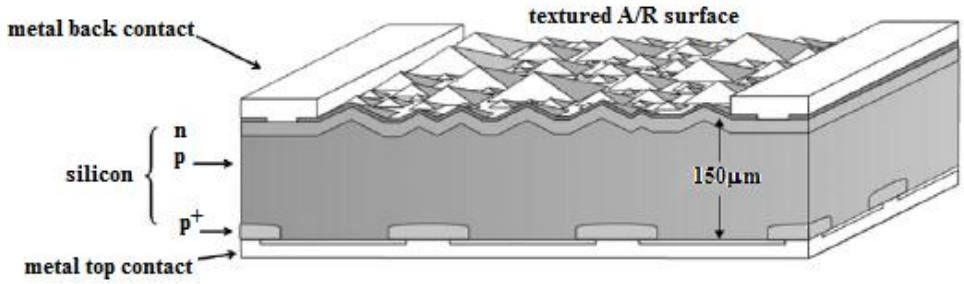

Figure 2.8 - Schematic of a single-crystal solar cell [Bagnall and Boreland, 2008].

According to Baur *et al.* (2007) and Green (2007), the purpose of thin film technologies for PV is to reduce cost and unnecessary material from the cost equation, using thin-film techniques to reducing the amount of light absorbing material. Different maximum efficiency records are achieved according to the thin-film technology used. In Figure 2.9, it is possible to find 18% of efficiency for Cadmium Telluride (CdTe) cells, a record of 20.3% efficiency for Cooper-Indium-Gallium-Selenide cells [ZWS, 2010] and 12.5% efficiency for amorphous-Si cells. Commercially available solar cells using these technologies achieve lower efficiencies: 11% (First Solar) [Kho, 2008], 10% (solyndra) [Wang, 2008] and 10% (Oerlikon) [Oerlikon Solar, 2010] respectively.

MJ cells are another kind of cells with a much higher efficiency potential than any other technology, and consists of multiple semiconductors, each of them capable of absorbing in a different region of electromagnetic spectrum, thus improving largely their performance.

The complexity of the materials used on these cells, such as Gallium arsenide (GaInP), Germanium (Ge), Indium phosphide (GaInP) makes the fabrication extremely expensive [Bosi and Pelosi, 2006]. To reduce the cost per watt it is thus necessary to increase the concentration factor to very high values (at least 100x, often >500x) in order to dilute the cell cost on the overall system cost.

Recently, Gutter *et al.* (2009) from Fraunhofer Institute for Solar Energy Systems (ISE) announced a new record efficiency of 41.1% for a MJ cell made of GaInP/GaInAs/Ge, as shown in Figure 2.9.

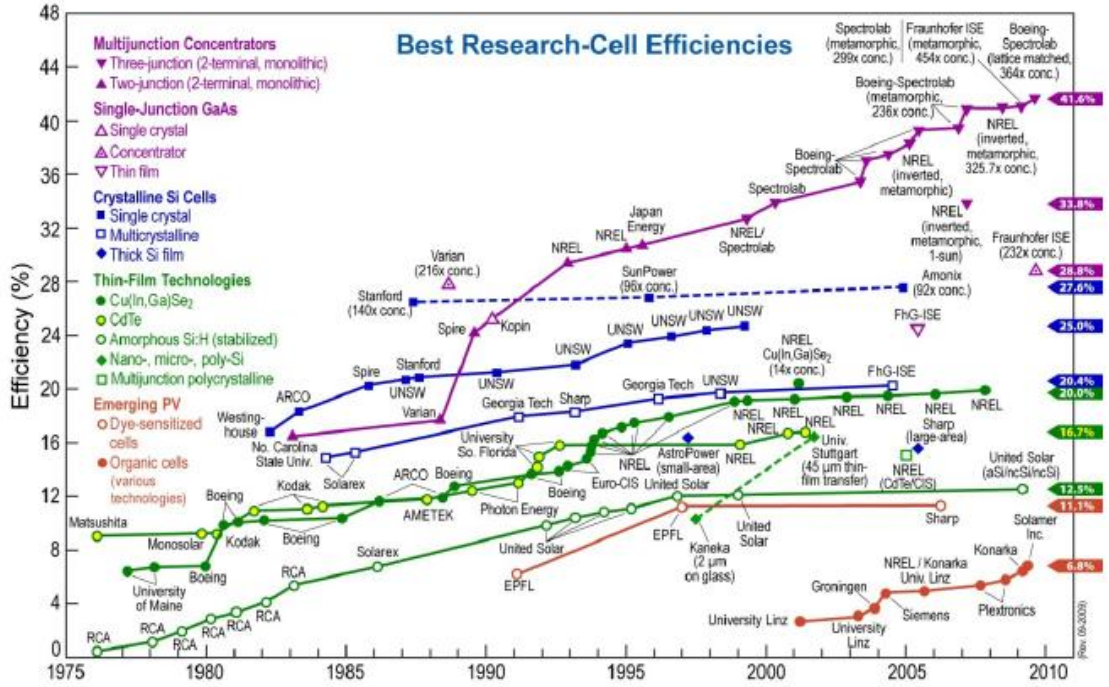

Figure 2.9 - Historic summary of champion cell efficiencies for various PV technologies. [Kurtz, 2009].

2.4 Solar cell parameters

A solar cell may be represented by the diode equation. Its electrical characterization is usually realized through its Current-Voltage (*I-V*) curve (Figure 2.10).

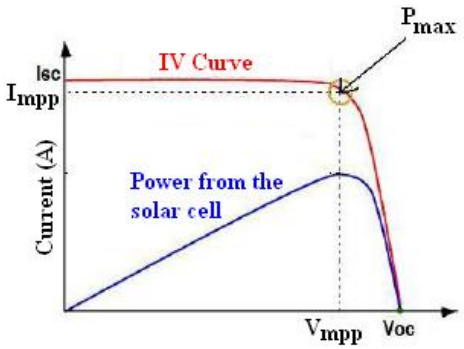

Figure 2.10 – IV curve representation.

The most relevant electrical parameters are:

i. Open circuit voltage (V_{OC}) is the maximum voltage available from a solar cell, which occurs when I=0; it is given by expression 1 and it decreases with temperature increasing.

$$V_{OC} = \frac{nKT}{q} \ln\left(\frac{I_L}{I_0} + 1\right) \quad (1)$$

ii. The short-circuit current (I_{SC}) is the current through the solar cell when V=0 (i.e., when the solar cell is short circuited). It depends directly on short circuit current density (J_{SC} in mA/cm^2) and cell area (A_{cell} in cm^2) (expression 2). The higher the light intensity the higher will be I_{SC} . It is also influenced by absorption and reflection of the solar cell.

$$I_{SC} = J_{SC} \times A_{cell} \quad (2)$$

iii. Fill Factor (*FF*) determines together with V_{OC} and I_{SC} the maximum power from a solar cell as showed by expression 3.

$$FF = \frac{I_{mpp} \times V_{mpp}}{I_{SC} \times V_{OC}} \quad (3)$$

iv. The efficiency of a solar cell is determined as the fraction of incident power which is converted to electricity and is defined by expression 4:

$$\eta = \frac{V_{OC} \times FF \times I_{SC}}{G} \quad (4)$$

v. Maximum power system is defined by expression 5:

$$P_{\max} = V_{OC} \times I_{SC} \times FF \quad (5)$$

3. Encapsulating materials and methods for PV modules

The goal of the encapsulation is to protect the solar cells from physical, chemical and mechanical damages in order to provide a high electrical reliability. Additionally [Czanderna and Pern, 1996] has highlighted the following requirements of the encapsulation:

i. To provide structural support and positioning for the solar cell circuit during fabrication, handling and operation;

ii. To achieve and maintain good optical coupling;

iii. To provide physical isolation of the solar cells and circuit components;

iv. To efficiently deal with high temperatures and temperature fluctuations.

The encapsulation process for a conventional PV module is called lamination. In a PV module, lamination is an assembly of electrically interconnected solar cells enclosed in two polymeric encapsulant foils, usually Ethylene Vinyl Acetate (EVA), a weatherproof package made of glass and the backsheet which is used to protect the system from environmental conditions. Figure 3.1 illustrates an example of a conventional PV module and its components.

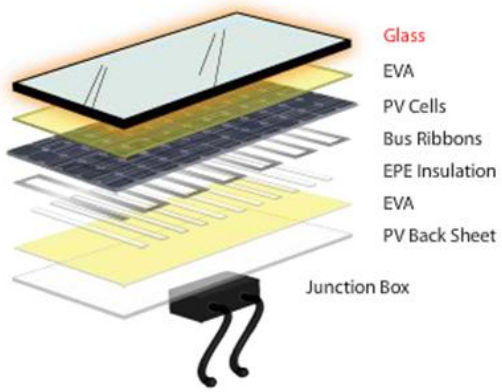

Figure 3.1 - Example of the most common PV module constituent's configuration before lamination. The interconnected cells are stacked inside two EVA foils with glass as frontsheet and a polymeric layer as backsheet [Dunmore, 2010].

3.1 PV encapsulation process

The vacuum lamination process is the most common encapsulation method for the PV industry. Usually the vacuum laminators consists of a double-sectioned "picture frame" enclosed at the top with a metal plate and a heated plate at the bottom where a flexible diaphragm separates the upper and lower chambers, as shown in Figure 3.2. A good laminate stack requires an uniform and continuous heat distribution at the different process stages.

(a) **(b)**

Figure 3.2 – a) Spire vacuum laminator where lower and upper chambers are visible. b) Enlargement of upper and lower chambers in the Spire vacuum laminator [Spire Solar, 2010].

Both chambers allow for controlled air evacuation and return to atmospheric conditions. While the top chamber is permanently fixed, the bottom chamber is only sealed upon closure of the laminator, i.e. the bottom portion of the picture frame contacts the heated plate over a silicone rubber gasket to form an airtight seal. It is within this bottom chamber that the PV module lamination occurs [Spire Solar, 2010]. Figure 3.3 is a representation of a conventional manufacturing PV module line.

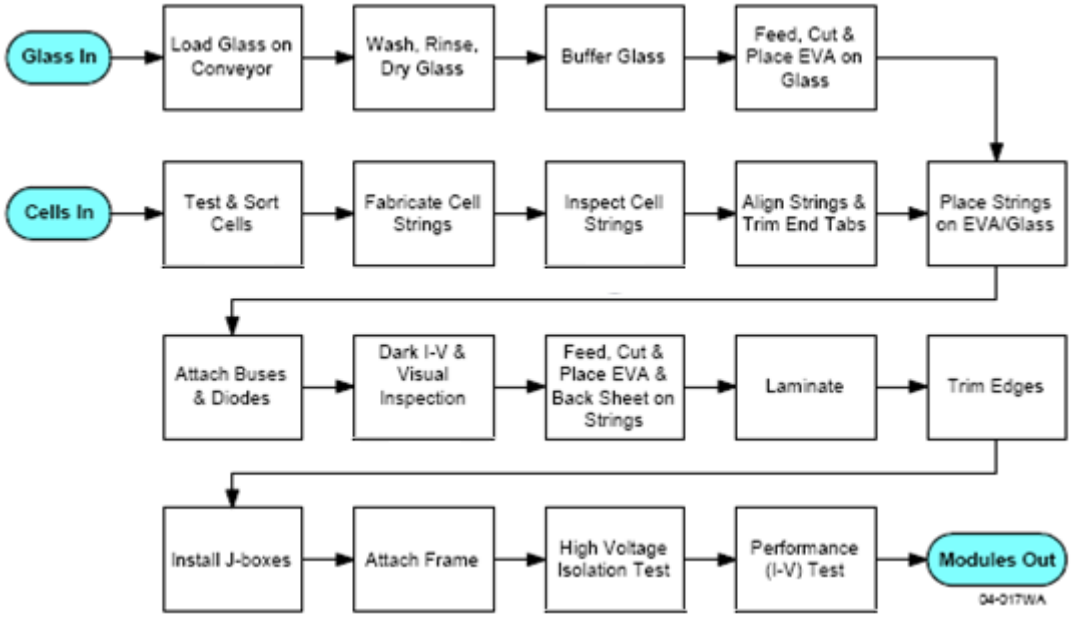

Figure 3.3 – Brightfield module line process flow chart [Nowlan, 2007].

3.1.1 Vacuum lamination process

The lamination processes depend on the properties of the materials and the equipment used. For the optimization of the encapsulation process, the target is to determine the shortest sequence which produces a good lamination without negative effects to any of the laminate components [Amrani *et al.*, 2007].

The most critical step of the lamination cycle is the step prior to plastic melt of the sheet encapsulant. The amount of time the assembly is under vacuum, the time at which pressure is applied, the temperature when pressure is applied, and the duration and quantity of pressure are all factors that affect the quality of the lamination.

Since the polymerization reaction (also called *crosslinking* reaction) is irreversible. A homogeneous thermal treatment step is crucial in the solar cells encapsulation process to assure the quality control of

the device. If a default happens during the polymerization (e.g. break, short circuit, string moving), the module quality will be lost.

Figure 3.4, shows a lamination process described by Amrani *et al.* (2007). The process starts with the introduction of the laminate stack (cells and the encapsulant materials) in the lower chamber where the temperature is kept constant at 100°C. The upper chamber is kept under vacuum (0.133 mbar).

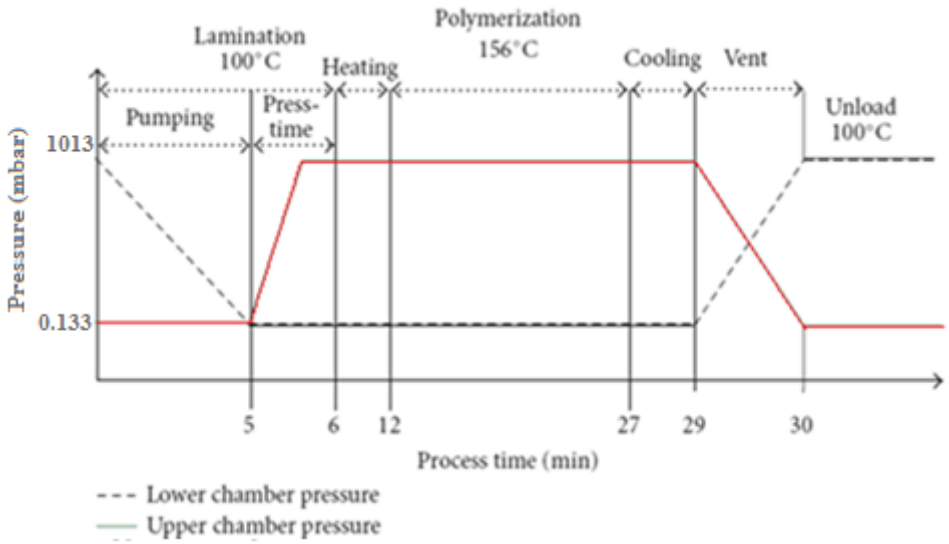

Figure 3.4 - Thermal treatment profile (long cycle) in the laminator [adapted from Amrani *et al.*, 2007].

In *Lamination* the air inside the lower chamber is removed during 5 minutes. The pressure is then set at 0.133 mbar and maintained during both the lamination and the polymerization cycles. Second, the upper chamber is filled with air to provide pressure on the module. During this phase, the combination of the lower chamber air-pumping and the pressure applied by the membrane allows to drive out the residual air and moisture that might be present in the laminate.

In *Polymerization* **t**he module is heated and the EVA melts the surrounding electrical circuits forming seals in front and back of the cells. The curing is done at 156ºC during 15 minutes. The EVA is crosslinked forming a chemical bond hermetically sealed around the module components.

Cooling is performed at 100ºC, the lower chamber is at the atmospheric pressure and the upper chamber is at 0.133 mbar.

3.1.2 Frontsheet – Glass

The HSUN concept, as well as other CPV concepts, does not include a frontsheet of glass. However, for completeness when describing the typical industrial encapsulation process, this section briefly discusses the most relevant technological issues and challenges for glass frontsheets for PV modules.

There are two glass classes in PV industry: low iron float glass and low iron patterned glass.

Low iron float and patterned glass

The low iron float glass is also named ultra-clear glass. Pilkington (2009) has described the most common low iron float glass manufacturing process. Compared to normal float glass, it has higher optical transmittance, lower reflectance, higher mechanical strength and the higher flatness.

The low iron patterned/textured glass is made by a continuous roll-impressed process. The textured surface of this glass may increase the efficiency of the PV module, in particular for static applications [Saint-Gobain Solar, 2010].

Composition

Low iron glass formulations have varied over the years. The glass industry has found formulations that appear to be a good tradeoff between encapsulant protection and the loss of usable light to solar cells.

Table 3.1, shows the manufacturing materials used at Saint-Gobbain Solar Glass. Worth notice is the low iron content of the used materials, such as soda, silica sand, dolomite, feldspar, and limestone.

Table 3.1 – Low iron glass row materials.

Component	% (w/w)
Silica Sand	58,1 %
Soda	18,9 %
Dolomite	14,7 %
Limestone	5,9 %
Aluminium hydroxide	1,0 %
Feldspar	0 %
Sulphate	1,0 %
Antimony trioxide	Max. 0,3%
	99,9 %

Note: The values displayed in this table were supplied directly by Saint-Gobbain Solar Glass.

According to Directive 2002/95/EC, of 27th January 2003, the European parliament legislates about the restriction of the use of certain hazardous substances in electrical and electronic equipment, such as PV modules. Table 3.2 shows some of the harmful components, such as heavy metals (lead and mercury), that must be avoided in PV glass manufacturing in order to prevent environmental contaminations.

Table 3.2 - Harmful components in PV glass industry according with legislation.

Component
Lead (Pb) or lead-based preparations
Mercury (Hg) or mercury-based preparations
Bromine (Br)
Dibutyl phthalate
Chlorinated hydrocarbons
Phenol compounds
Organic tin compounds

Tempered glass

Both low iron glasses described previously can undergo through a heat treatment. Low iron float and patterned tempered glass may be processed in a tempering oven at around 650ºC, then quenched with air jets so that the surfaces are cooled faster than the inside core. At room temperature, the core will continue to cool.

Some of the features of tempered glass are:

i. Increase its strength to resist to mechanical impacts and increase the thermal resistance; it is approximately four times stronger than non-tempered glass of the same thickness and configuration;

ii. When the glass breaks, the core releases tensile energy resulting in the formation of small and safer glass particles representing a security advantage when compared with the normal annealed glass.

Cerium doped glass with UV filtering

Module superstrate materials are required to have high spectral transmittance for all wavelengths of sunlight to which photovoltaic cells in the module respond. However, one important tradeoff has to do with the transmittance of short-wavelength ultraviolet (UV) sunlight.

Typically, the polymer encapsulants used to laminate the superstrate to the solar cells in a module are degraded by extended exposure to UV light. Therefore, it is desirable for the module superstrate to prevent ultraviolet sunlight (< 400 nm) from reaching the encapsulant material. To screen out ultraviolet (UV) light, a small amount of the element cerium (Ce) can be added to glass formulations used for PV modules.

Rejection of the infrared (IR) sunlight is another optical characteristic that would raise module performance and increase module lifetime by reducing operating temperatures. However, a cost-effective method for rejecting the infrared heat has not yet been developed.

Figure 3.5 shows in detail the existing UV regions, *UV-B*, *UV-AII* and *UV-AI*, which extends from 290-320 nm, 320-340 nm and 340-400 nm, respectively. In polymeric based encapsulant materials *UV-B* is the region of the solar spectrum that originates the most degradation damage [Kempe *et al.*, 2009]. An incoming advantage from the use of low iron glass doped with Cerium is the reduction of transmission in UV-B region, as clearly shown in Figure 3.5.

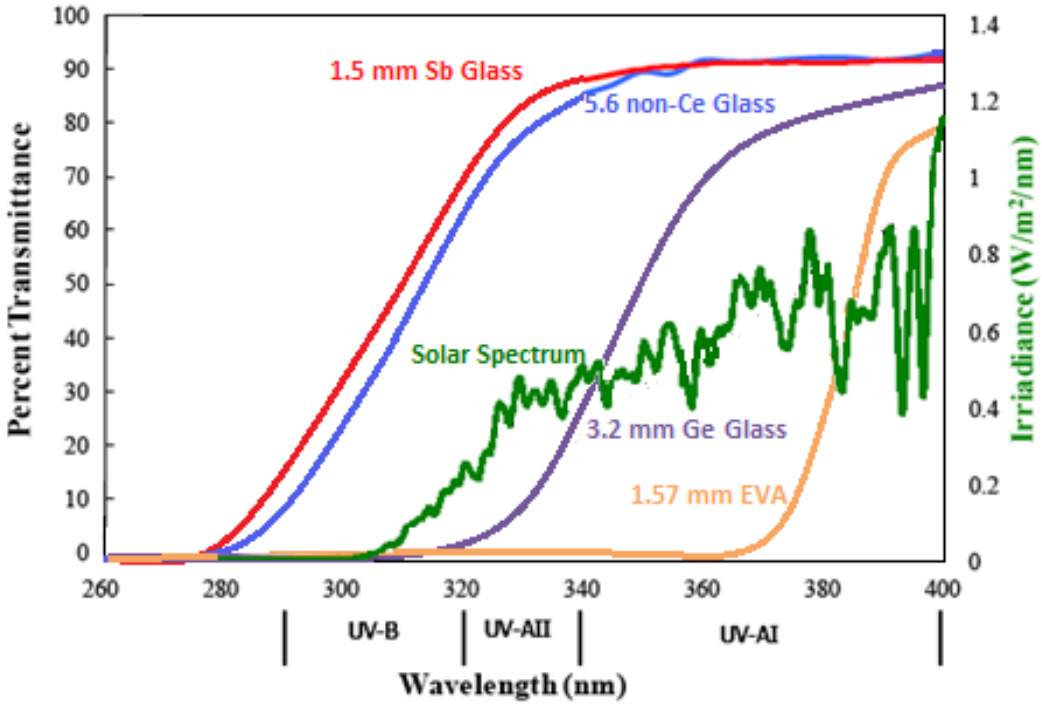

Figure 3.5 - Comparison between the AM 1.5 global solar Spectrum and the effect of Ce-glass, non-Ce glass, a laminate construction of 3.2mm Ce glass/1.57 mm EVA/3.2mm Ce glass, Antinmony (Sb) glass [adapted from Kempe *et al.*, 2009].

However, the use of glass doped with Ce can be problematic. In typical low-Fe Ce-doped glass, the Ce is present in both the Ce^{3+} and Ce^{4+} states. It is the Ce^{3+} state that absorbs UV light with peak absorption around 314 nm. Upon exposure to UV radiation, the Ce^{3+} will be oxidized to the Ce^{4+} state. Because diffusion of oxygen into soda lime glass occurs on geologic time scales, Ce cannot be oxidized without a corresponding reduction reaction. In glass containing iron, Fe^{3+} will be reduced to Fe^{2+} as,

$$Ce^{3+} + Fe^{3+} \xrightarrow{\text{UV Light}} \underset{\text{Less Light Transmission}}{Ce^{4+} + Fe^{2+}} \qquad \text{(C.R. 1)}$$

Unfortunately, Fe^{2+} has a broad absorption peak around 1050 nm, which is within the useful range of typical silicon based PV technologies. Fe^{3+} has a relatively weak absorption peak in the UV range around 370 nm. Thus, "solarization" results in a small decrease in PV performance upon field exposure of Ce-containing glass [Kempe *et al.,* 2009]

Adding small amounts of Sb during float glass manufacturing can prevent Ce problem. During this addition Fe^{2+} is oxidiezed to Fe^{3+} creating a very high transmittance glass that has a slight yellowish appearance rather than a typical green colour.

$$Sb^{5+} + 2Fe^{2+} \rightarrow \underset{\text{High Photon Transmission}}{Sb^{3+} + 2Fe^{3+}} \qquad \text{(C.R. 2)}$$

However this process will also result in the oxidation of the UV absorbing Ce^{3+} ion resulting in high UV transmission.

$$Sb^{5+} + 2Ce^{3+} \rightarrow \underset{\text{Low UV absorption}}{Sb^{3+} + 2Ce^{4+}} \qquad \text{(C.R. 3)}$$

For this reason, the use of Sb to promote high optical transmission is not compatible with the use of Ce to block UV transmission.

3.1.3 Backsheets

The use of the backsheet in a PV module has several purposes which contribute for the PV modules functionality, longevity and safety of people who work with or near the module. Some of these purposes are:

i. Increase mechanical protection. Tensile strength and elongation represents the maximum stress that a material can withstand before necking and affect its characteristics irreversibly. This property depends directly on the lamination process. Peel strength is a measure to quantify the backsheet-encapsulant adhesive bonds and can be performed at 90º and 180º.

ii. Low interface thermal conductivity to dissipate heat flow;

iii. Electrical insulation capacity is represented as the breakdown voltage that is a quantitative measure of an insulator when electrically conductive;

iv. High dielectric performance and maximum system voltage grants a good electrical insulation to the system (According the IEC partial discharge test measured by TUV, in Europe it is necessary to perform 1000VDC);

v. Increase the resistance to UV irradiation;

vi. Water Vapour Transmission Rate (WVTR) is the ability to avoid moisture entrance in PV module, at all temperature range. For flat panels WVTR< 2 g/m^2day and thin film WVTR < 0.05g/m^2day;

vii. Dimensional stability represents the ability of the material to handle moisture, thermal expansions and other stresses. For PV applications, this property should be as lower as possible, usually less than 1%. It also depends on the lamination process;

viii. Relative Thermal Index (RTI) is the ability of a material to support temperature without lost of its properties and should be as higher as possible.

As an alternative to glass, it may be interesting to incorporate polymeric backsheets in PV modules. These constructions can eliminate glass breakage and provide a more durable mechanical package. In addition, lighter weight can be more cost effective.

The conventional backsheet material (Figure 3.6) is composed by Tedlar or polyvinyl fluoride (PVF) and polyethylene terephthalate (PET) which ensures electrical insulation, durability, low flame spread, material strength, resistance to hydrolysis and UV light [Richard, 2010].

Figure 3.6 – Backsheet from Dupont^{TM} with Tedlar-PET-Tedlar [DuPont, 2010].

Dupont is the Tedlar manufacture and represents about 2/3 of the market. However, with Dupont failing to supply sufficient quantities the costumers needs for during growth periods, module manufactures have been looking for alternatives to avoid such strong market dependence. Section 4.1 lists the existing manufactures and products.

3.1.4 Encapsulant Requirements

Encapsulant materials should provide several functions to the system, such as a reliability of 20-30 years and a maximum power loss performance of 20% over a 20 years period [Czanderna and Pern, 1996]. Polymeric based encapsulants, such as EVA, have elastomeric properties that deal with different material thermal expansions, in order to avoid over-stressing and cracking.

Polymeric based materials are typically lighter weight, cost less, are easier to process, and are more conveniently assembled than most inorganic and metallic materials. They offer a number of economic and performance advantages as a pottant in PV modules [Gebelein *et al*., 1983; Cuddihy *et al*., 1986].

Czanderna and Pern (1996) and Agroui *et al*. (2007) have identified the most important properties of the encapsulants:

i. High temperature stability;
ii. High UV resistance;
iii. Low thermal resistivity;
iv. Good adhesion to different module materials;
v. High optical transmittance.

The most important bulk properties of an encapsulant are its chemical, mechanical, optical and electrical properties, as shown in Figure 3.7.

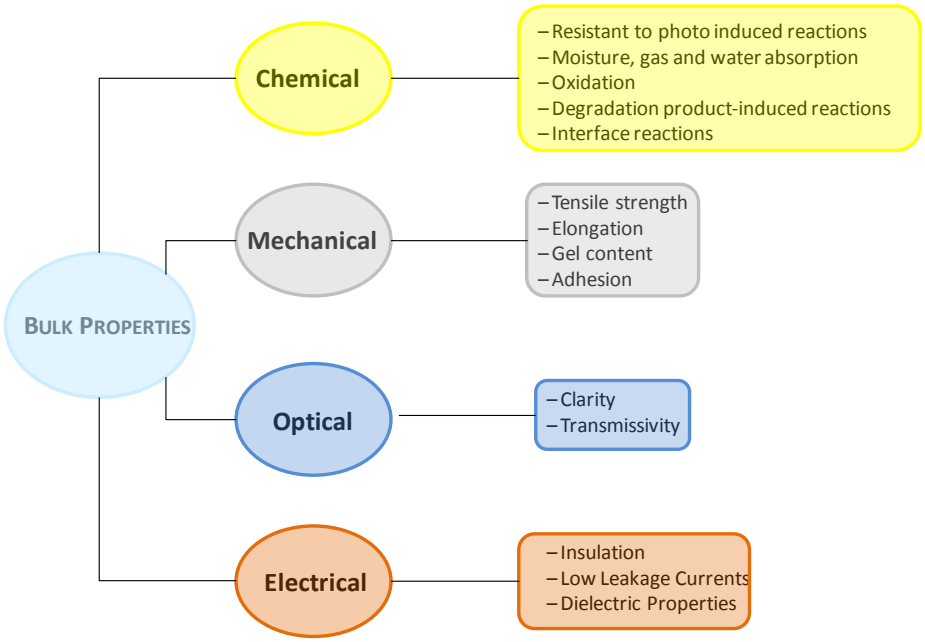

Figure 3.7 – The most important bulk properties of an encapsulant.

Each of these bulk properties is affected in different ways by solar irradiation, thermal and humidity cycles. When choosing an encapsulant, these properties should be thoroughly assessed.

Some of the problems that can occur if the encapsulant is not the adequate are yellowness, bubbleness, module break, loss of efficiency, etc.

3.2 EVA – Ethylene VinylAcetate

EVA is the most extensively used polymeric encapsulation material for conventional modules in the PV industry. This section briefly describes its most relevant properties as an encapsulant material.

3.2.1 What is EVA

The chemical structure of EVA is shown in Figure 3.8. The transparent EVA copolymer, formulated with stabilizers, was developed by Jet Propulsion Laboratories (JPL) and Springborn Laboratories in early 1980's [Czanderna and Pern, 1996] and has been predominantly used by the PV industry since then.

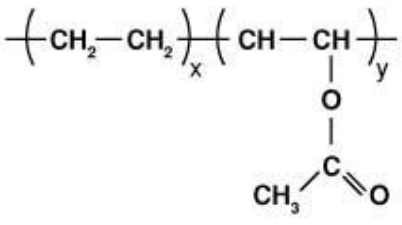

Figure 3.8 – Chemical structure of EVA copolymers.

The placement of the EVA depends on the technology used. As mentioned above, the conventional PV module based in crystalline silicon cells typically uses a glass/pottant/solar cells/ pottant/ backsheet configuration (Figure 3.9). Inadequate or defective packaging, aging behavior and degradation mechanisms can be the predominant cause of failure in PV modules [Czanderna and Pern, 1996; Allen *et al.*, 2000; Rodriguez-Vázquez *et al.*, 2006; Kempe *et al.*, 2007].

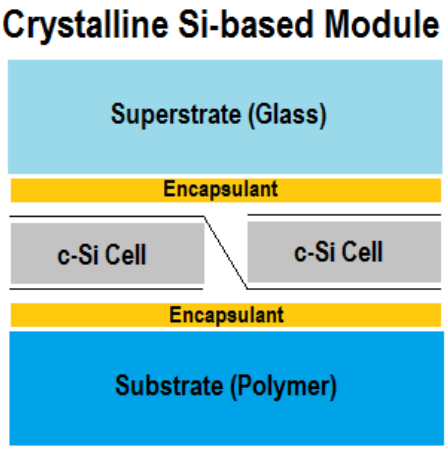

Figure 3.9 – Typical PV module encapsulation configuration with EVA as pottant [Pern, 2006].

Czanderna and Pern (1996) lists the main requirements for encapsulants and especially for EVA (Table 3.3). For example, the light transmission within the relevant spectrum should be higher than 90%.

The tensile strength of these encapsulants should be lower than 20.7 MPa to avoid breakage and also should not presents UV degradation at wavelengths higher than 350nm. In order to avoid collateral reactions, the water absorption of the encapsulant must be lower than 0.5 wt%.

Table 3.3: Specification and requirements for compounded EVA pottant materials. [Adapted from Czanderna and Pern,1996].

Characteristic	Specification or requirement
Glass transition temperature (Tg)	< -40°C
Light transmission (400<λ<1000 nm)	> 90% of incident
Hydrolysis	None at 80ºC, 100% RH
Water absorption	< 0.5 wt% at 20ºC / 100% RH
Resistance to thermal oxidation	Stable up to 85ºC
Mechanical creep	None at 90ºC
Tensile strength	< 20.7 MPa (<3000 psi) at 25ºC
Fabrication temperature	≤ 170ºC for either lamination or liquid pottant system
Fabrication pressure for lamination pottants	≤ 1 atm
UV absorption degradation	None at wavelength > 350 nm
Hazing or clouding	None at 80ºC, 100% RH
Minimum thickness on either side of solar cells in fabricated modules	0.152 mm
Toxicity	None

To inhibit degradative reactions, some additives are added to the usual EVA. Table 3.4, shows an EVA formulation of Dupont trademark for a typical cure.

Table 3.4 - Usual EVA formulation [Adapted from Czanderna and Pern, 1996].

Component	% (w/w)
EVA copolymer	97,943
UV absorver	0,294
UV stabilizer	0,098
Anti-oxidant	0,196
Curing agent	1,469

Note: Ethylene vinyl acetate copolymer is a mixture of 67%(w/w) of ethylene and 33%(w/w) of vinyl acetate.

EVA is mainly available in three types: Standard cure (SC), Fast Cure (FC) and Ultra Fast Cure (UFC). Each type is determined according to the type of curing agent.

In order to increase throughput of the lamination process, the fast or ultra-fast cure formulations are more common since FC materials can achieve higher throughputs due to a reduction of almost 40% of the lamination process [Richard, 2010]. A comparison between different lamination and required times is presented in Table 3.5.

Table 3.5 – Comparison between the lamination/cure times for standard, fast and ultra fast cure EVA [adapted from Specialized Technology Resources, 2010[A]].

Cure Type	Standard Cure	Fast Cure	Ultra Fast Cure
Plate temperature	150°C	150°C	175°C
Vacuum pump time (pump-down cycle)	4 min	4min	4min
Lamination Time (press cycle)	2 min	8 min	3.5min
Oven temperature	140°C	n.s.	n.s.
Oven cure time	24 min	n.s.	n.s.

n.s. – not supported

Note: Differences between EVA types were neglected. Referenced times are an estimation and always depends on gel content. Times and pressure/temperature ranges for the presented lamination are different from the noticed in Figure 3.4 due different EVA formulation

.

The degree of cross-linking (ability that one polymer has to link to another) is expressed as % of gel content. It depicts an indication of the polymer fraction that is not extractable (with a solvent, e.g.), thus it is the fraction that is cross-linked.

Gel content is influenced significantly by the lamination and curing cycle used during the module's manufacture. This parameter should be higher than 75% to improve the module longevity [Specalized Technology Resources, 2010[A]].

In a production line, EVA is subjected to gel content determination before undergoing to the lamination process. Percentage of gel content defines the time and temperature of the process (Table 3.6).

Table 3.6 – Time/Temperature/Percent Gel for fast-cure EVA [adapted from Specialized Technology Resources, 2010[A]].

Time (min)	Temperature (ºC)			
	130ºC	140ºC	150ºC	160ºC
2	0.0 %	73.4 %	81.5 %	84.2 %
5	60.3 %	83.7 %	88.6 %	91.0 %
10	75.0 %	88.2 %	91.6 %	92.3 %

High gel content (e.g., 100%) is not necessarily bad, as it implies that the entire polymer has been incorporated into the cross-linked structure, and not that all possible crosslinking of bonds have occurred. As long as the encapsulant remains soft and retains reasonable elasticity, the increased crosslinking presents no problem to the module's performance [Wohlgemuth and Petersen, 1991].

This testing is important, not only in the initial development of a lamination cycle, but for continued monitoring as well as to ensure that the process does not drift. An insufficiently cured module may experience cell movement, delamination or current leakage during wet hi-potential testing [Holley, 1995].

3.2.2 EVA Properties

Transmittance

Typically, optical properties are not changed by temperature variations or the application of stress. Still, the simultaneous variation of these properties can change the polymer morphology and consequently decrease the polymers clarity.

Figure 3.10 shows a light transmission spectrum of different EVA materials where it is visible the UV cut at the 360 nm. In the visible range, (400-1000 nm) EVA shows a transmission higher than 90%. It is interesting to notice how similar the different EVA products are as far as transmittance is concerned.

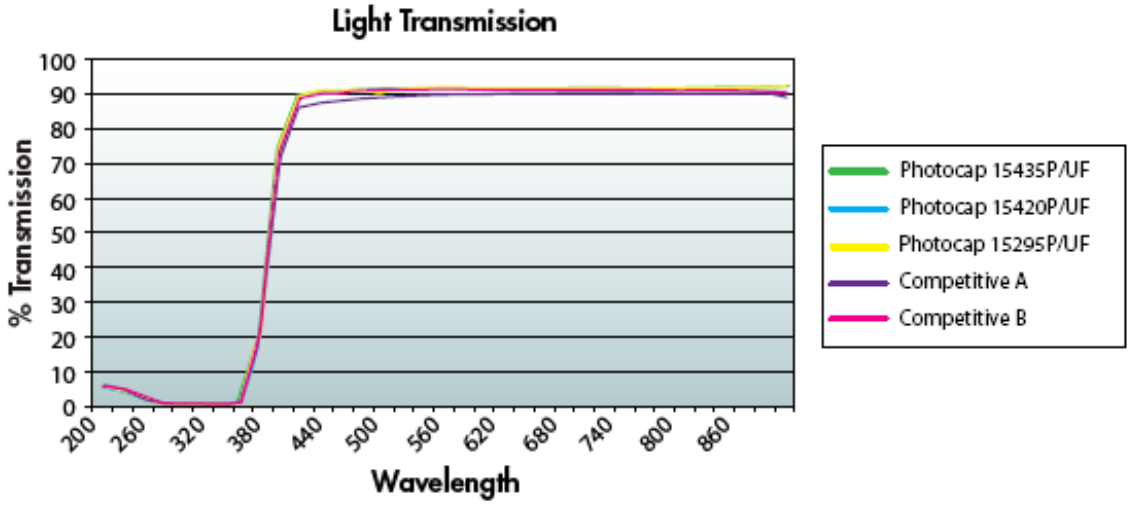

Figure 3.10 – Influence of transmittance through the UV-vis spectrum [Specialized Technology Resources, 2010[B]].

Adhesion

Adhesion tests should be performed to test the durability and the interfacial adhesion. In a PV module the following sets must be tested: EVA-Backsheet, EVA-EVA and EVA-Glass (or frontsheet). Cells are not an integrant part of this set because stays locked in the middle of the encapsulant. This test must be performed to avoid delamination during the device lifetime. Adhesion strength is influenced by the backsheet formulation and manufacturing source, glass type and surface priming on the glass surface or on the backfoil. Figure 3.11 illustrates peel strength adhesion test which contemplates 90º and 180º [Jorgensen *et al.*, 2006].

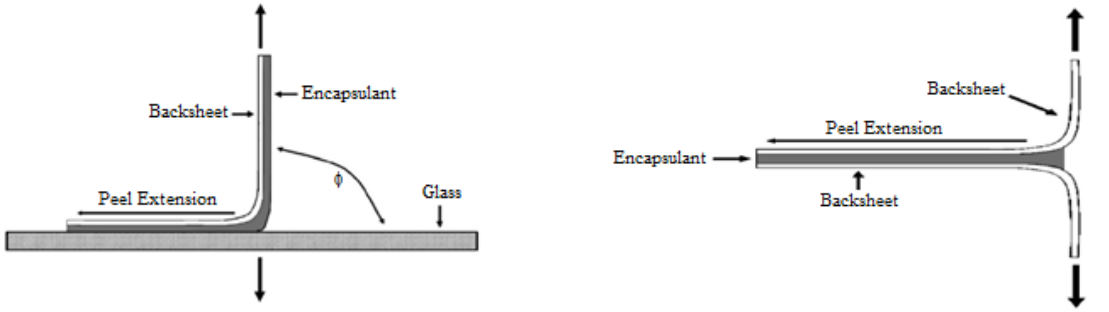

(a) **(b)**

Figure 3.11 – Adhesion tests performed during the choice of an encapsulant: a) Typical peel-strength measurement at 90º; b) T-peel strength measurement [Jorgensen *et. al*, 2006].

Adhesion tests are usually performed during the module lifetime tests such as damp heat exposure. A stress test applied to modules for several hours to predict delamination effects. Figure 3.12 shows an example of peel strength tests during such a damp heat test. In this case study, delamination occurred after 500 hours of testing for one of the used materials.

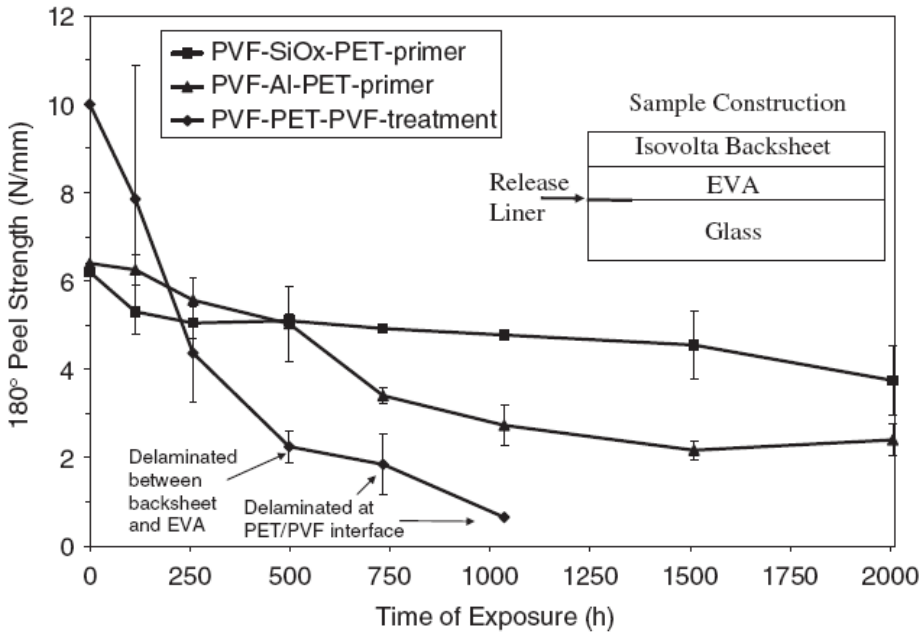

Figure 3.12 – Peel strength test in the EVA/glass interface, for PVF containing backsheets, as a function of damp-heat exposure [Jorgensen *et. al*, 2006].

3.2.3 EVA Degradation

Absolute stability is not a requirement to the service lifetime of the encapsulant. Instead, the rate of reaction and the relative stability are crucial to the lifetime of the device.

Stability can be measured through the overall effects of degradative reactions, the degradation mechanisms of EVA, photothermal reactions and the formulation used to stabilize EVA,

A poor relative stability is usually associated to ultraviolet (UV) irradiation of polymers which can bring three primary types of reactions:

i. Chain scission reactions that will lead to a reduction in the molecular weight, causing a loss in mechanical properties such as elongation at break and on the permeability, often leading to delamination and efficiency losses.

ii. Crosslinking reactions will increase the stiffness of the polymer resulting in a decrease in elongation to break. High levels of crosslinking will lead to embrittlement of the polymer.

Chain scissions and crosslinking reactions caused by UV irradiation can have a substantial influence in permeability.

Permeability is influenced by the mobility of the polymer chains and the strength of the interaction between the polymer and the penetrant. The mobility of the polymer can be affected by prolonged exposure to environmental stresses. The permeation rate of gases through glassy polymers increases with temperature. Delamination and efficiency loss are the most noticeable lost properties.

Photothermal reactions

Photothermal reactions where high temperature and UV light will lead to formation of several undesirable compounds like acetic acid (CH_3COOH), aldehyde (CH_3COH), Carbon Monoxide (CO), Carbon Dioxide (CO_2), and Methane (CH_4). These co-products can lead to yellowing, bubbleness and shrinkage of the EVA as well as degradation in its tensile strength and elongation at break. Evolution of acetic acid during thermal or photothermal degradation produces an autocatalytic effect in EVA yellowing [Pern, 1993].

If an effective UV protection is placed in EVA, restriction of co-products will be effective. A good lamination process is also essential to avoid this problem limiting water entrance and consequently minimize lateral reactions.

Shrinkage and Bubbleness

The possibility of shrinkage when the material is subjected to aggressive temperature ramping during lamination is an important property in the encapsulant choice.

Shrinkage is a phenomenon that leads to formation of bubbles inside the laminate stack and when subjected to UV radiation, creates a photothermal reaction and consequently the already mentioned co-products.

Usually, manufacturers increase the lamination process window (thermal process) and reduce lamination times to solve this problem. Figure 3.13 presents examples of shrinkage and bubbleness.

(a) **(b)**

Figure 3.13 – Examples of bubbleness and shrinkage: a) Bubbleness and shrinkage example. b) Air bubbles resulting from EVA shrinkage during lamination.

Figure 3.15 shows the effects of yellowing on the transmittance in the UV and the visible range. At 380nm, the transmittance decreases from 90% to 56%. The overall effect across the spectrum is even more dramatic. Discoloration can decrease the power output from a PV module from at least 10% to 13% [adapted Czandena and Pern, 1996].

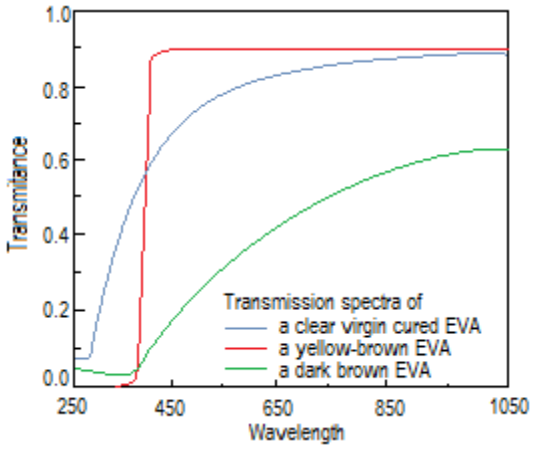

Figure 3.15 – Influence of yellowing in transmittance through the UV-vis Spectrum [adapted Czandena and Pern, 1996].

Moisture Influence

Moisture penetration and absorption by the primer blend in the encapsulant is responsible for the process of adhesion. Moisture attacks the coupling functional sites of the primer reducing its effectiveness.

Water can weaken interfacial adhesive bonds, resulting in delamination and ingress paths, which consequently results in loss of passivation, electrochemical corrosion and ultimately, device failure.

Performance of this test is essential to prove the reliability of the PV module and it is always dependent of the backsheet properties. Lamination process and products that avoid moisture entrance is the key to solve this problem [Kempe, 2006].

Delamination

When the materials are subjected to repeated cycles stresses, moisture and adhesion weakness can lead to electrical issues, corrosion, and bad electric contacts (Figure 3.16) it is shown a bad electric contact resulting from delamination.

Figure 3.16 – Delamination can cause these ribbons to open and get in short-circuit [Zgonena, 2010].

Dimensional properties

Dimensional properties are dependent of the lamination process. Tensile strength and elongation at break represents the maximum stress that a material can withstand before necking and affect its characteristics irreversibly.

Storage

Storage conditions can affect negatively the EVA adhesive strength. To prevent this from happening, EVA rolls should be stored in a clean room with controlled temperature and relative humidity. Table 3.7 represents the recommended conditions for storage. Storage at sub-freezing temperatures has not been found to result in any performance disadvantages.

Table 3.7 – Recommended Conditions to material storage.

Variable	Value
Relative Humidity (RH)	< 50%
Temperature	< 30°C (22ºC recommended)
Warranty	6 months

An example of adhesion weakness due to storage is given in Figure 3.17. Adhesion decreases linearly with time even when the samples are not exposed to sunlight.

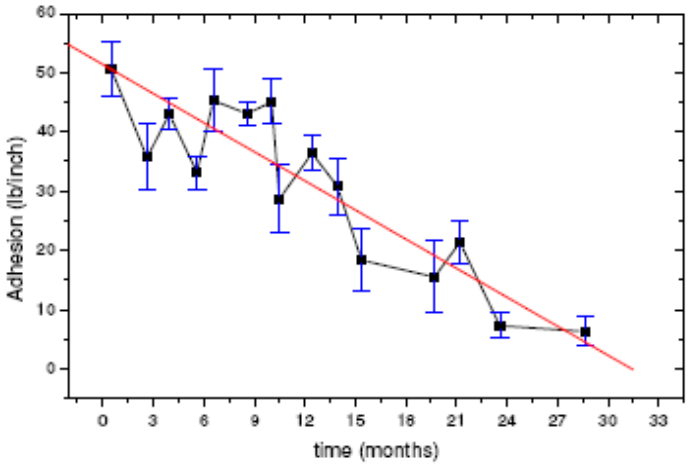

Figure 3.17 - Adhesion strength to glass as a function of storage time. Samples were stored at ambient conditions in 2 mil polyethylene bags in the dark [Specialized Technology Resources, 2010[A]].

Since EVA is extremely hygroscopic, it is sensitive to water. Additionally, it should not receive direct sunlight and should be always wrapped tightly with the original packaging. The outer layer of film should be discarded and the underlying layers should be used for module production because the additives tend to evaporate more at the edges and outside layers.

3.3 Silicone

Silicone polymers and resins have been formulated into multiple products that have a long history of successful use in a wide variety of applications.

In the PV module assembly market, silicones are an interesting material because of their excellent optical transparency over a wide spectrum and UV stability [Dow Corning Corporation, 1978] which makes silicones highly suitable for meeting the materials requirements for encapsulation of photovoltaic cells and other optic-electronic applications. However, pricewise silicones are still more expensive than EVA and therefore they are not widely used unless in CPV systems.

3.3.1 What are Silicones

Silicones for encapsulation purposes are mainly composed by Polydimethyl Silicone (PDMS) and presents differences in the chain numbers (Figure 3.18). The main reason for silicone demand increase is that is the only encapsulant that does not bear a carbon backbone. Therefore, this polymer is characterized with an high stability which is explained considering the energy of chemical bonds present in its chain (Si-C and Si-O). The lower silicon electronegativity (1.8) vs. carbon (2.5) leads to a polarised Si-O bond, highly ionic and with a large bond energy, 452 kJ/mole when compared to the Si-C bond, with a bond energy of ±318 kJ/mole. These values partially explain the stability of silicones [Colas, 2005].

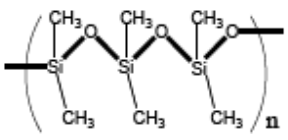

Figure 3.18 – Chemical structure of Polydimethyl silicone. Letter *n* represents the chain number.

The silicone encapsulants for PV applications are liquids composed by two parts: the base (Part A) and the curing agent (Part B).

Depending on the encapsulant, different proportions can be added (e.g., 10:1, 9:1 or 1:1). After adding the two parts, the mixture must be stirred (as slow as possible) to allow cross-linking reaction while avoiding air entrance. After the mixing, degasification vacuum application may be required. The mixture is then subjected to heat.

Therefore, comparing to the standard EVA lamination process, there exist some process advantages in silicones resulting from this cure process:

i. Cure process can be accelerated by heat, improving production lines;

ii. Viscosity allows an easy flow to complex parts covering totally the cell, providing excellent electrical insulation and shock resistance;

iii. Chemical composition contains no solvents for use on production lines presenting no corrosive by-products. EVA contains the ethylene and vinyl acetate.

iv. Silicones can be repaired during the module lifetime. A new liquid mixture can be added covering the silicone damage.

3.3.2 Silicone Properties

Silicones are an ideal product family to meet the needs in the PV module assembly market.

Transmittance and absorption

Silicones are highly transparent in the UV-visible wavelength region which makes them ideal candidates for cell encapsulants.

Figure 3.19 shows the relationship between a development product PV6100 and a non-specified EVA type in *UV-Vis* region. It is clear the higher transmittance of silicones when compared to EVA for the same thicknesses, in particular in the UV region.

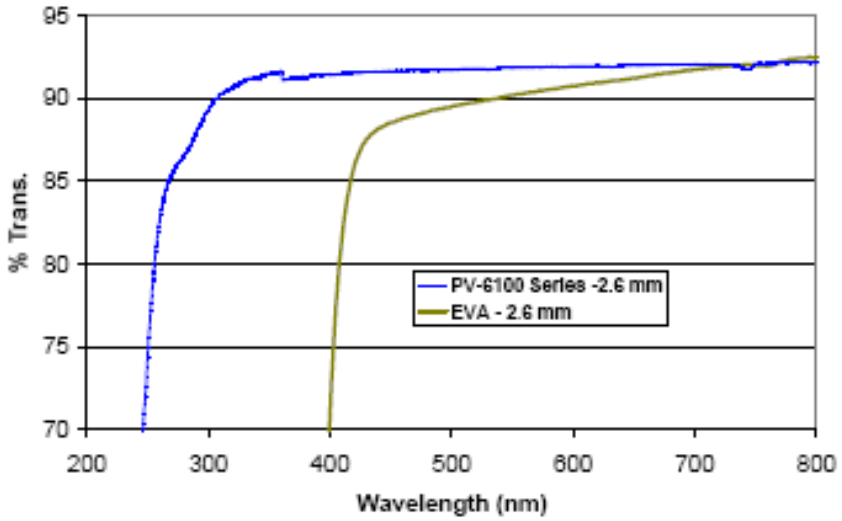

Figure 3.19 – Comparison between a two part silicone elastomer from Dow Corning and a non-specified EVA type [Ketola *et al.*, 2008].

The transparency of silicones to UV radiation increase their lifetime under insulation. Figure 3.20 shows that silicones only become opaque to wavelengths below about 300nm (compare to 400nm for EVA). However, for these wavelengths, if the frontsheet were low iron glass, the glass absorption would quench these UV photons further increasing the lifetime of the module.

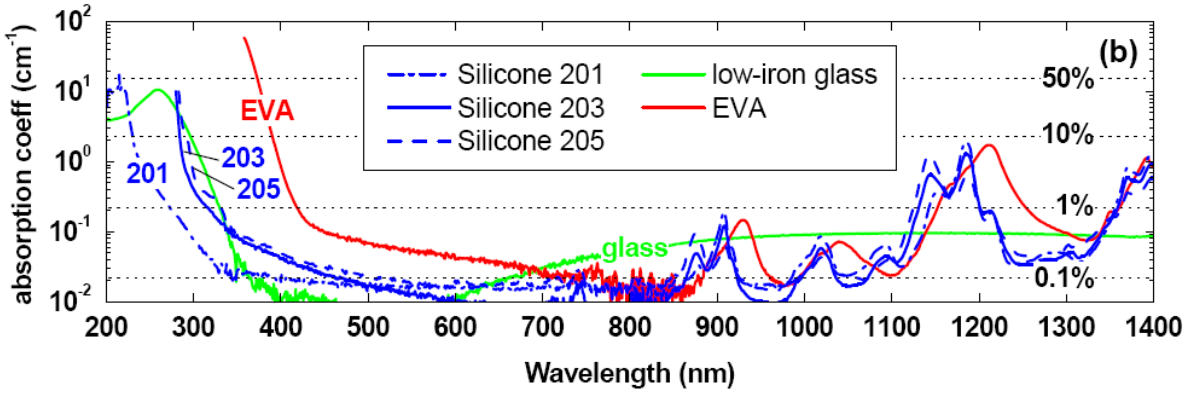

Figure 3.20 – Absorption coefficient for Dow Corning silicones and comparison with low iron glass and EVA [McIntosh *et al.*, 2009].

Figure 3.21 shows a study where silicone encapsulant is exposed to 30suns concentration during 132days. Absorbance does not present significant losses, yellowness and bubbleness are not present.

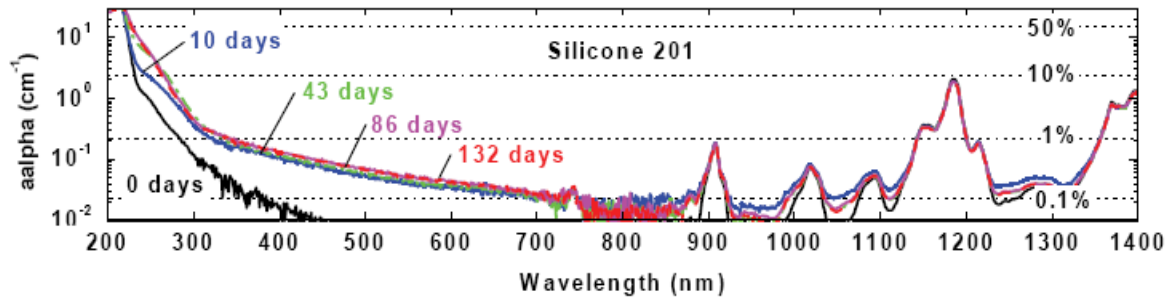

Figure 3.21 – Dow corning silicone after 132 days in a 30 suns concentrator [Kang *et al.*, 2010].

Mechanical properties

Young modulus (tensile modulus) is a measure of the stiffness of a material. It is defined as the ratio of the stress over the uniaxial strain measured in pressure units. Silicone encapsulants are formulated to be stress relieving, and for that reason, in Figure 3.22 presents a lower value when compared to EVA. This comparison shows that EVA is subjected to a higher stress during thermal cycles decreasing tensile strength properties.

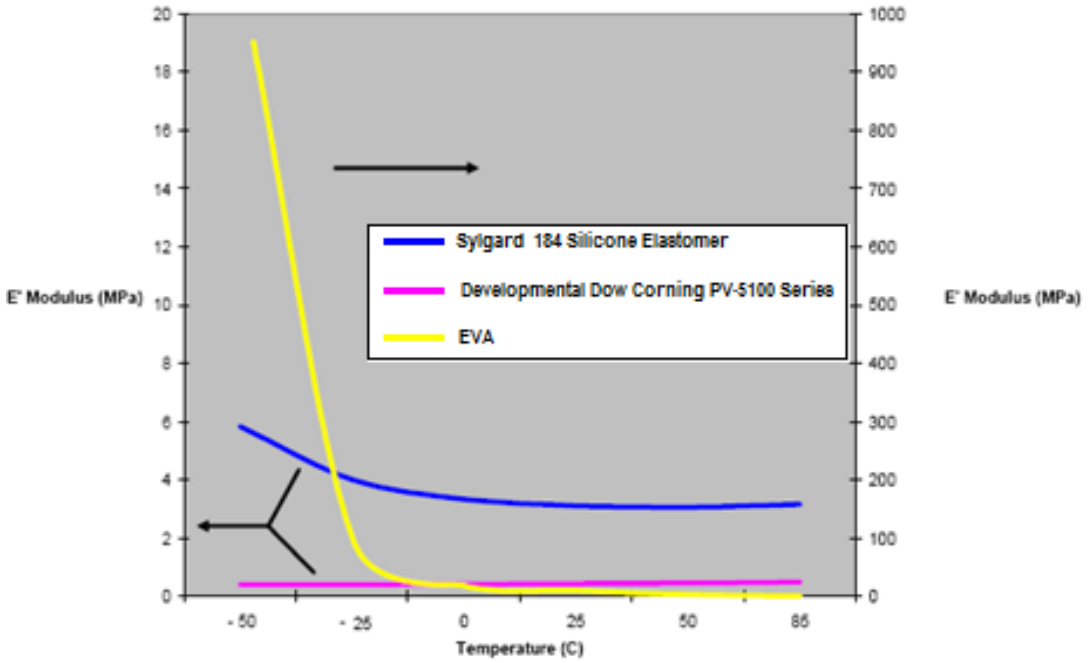

Figure 3.22 – Stress modulus variation as a function of temperature for EVA and silicone sample. Notice the different vertical scales [adapted from Ketola *et al.*, 2008].

Hardness

Elastomers encapsulants are extremely resistance to high temperatures, preserving their mechanical properties during extended times (Figure 3.23). Silicones can withstand continual changes in temperature caused by the heating up and cooling down of exposure to sunlight.

Among the most important properties of the vulcanizate are the mechanical and electrical values. Apart from the indentation hardness, usually quoted on the Shore A/Shore 00 scale.

The hardness of cured printing pads or silicone gels is too low to allow measurement of the Shore A hardness. For silicone gels, the Shore 00 indentation scale is used. Whereas for both Shore 00 and Shore A hardness, higher values mean greater hardness, for penetration the reverse is true: the higher the value, the softer the vulcanizate.

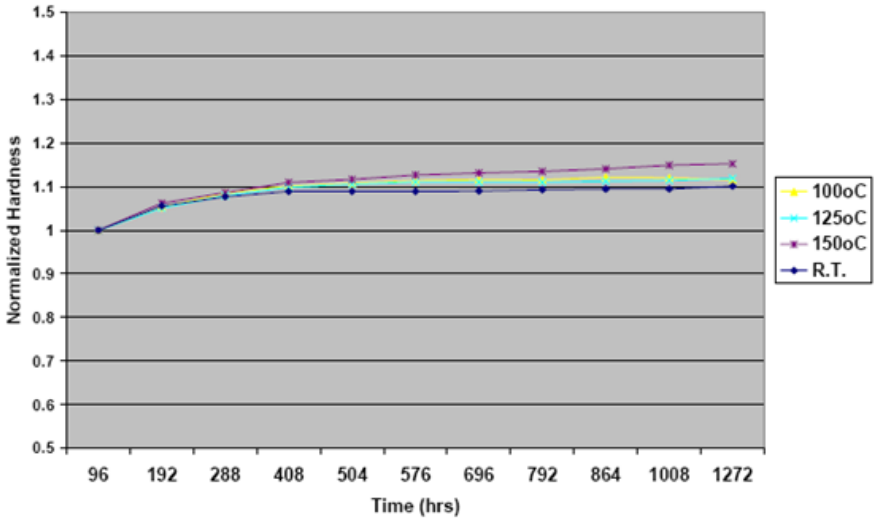

Figure 3.23 – Thermal stability of silicones in extended exposure at high temperatures [Ketola *et al.*, 2008].

Consistency

The viscosity of the material describes approximately its flow characteristics under intense shear, for example during metering, extrusion, stirring, etc. The higher the viscosity number, the more viscous the pourable compound or the stiffer the spreadable paste. Silicone gel and encapsulants presents different viscosities values (<1000 and ≈ 4000 mPa.s[1], respectively).

Metering the Components

It is absolutely essential to meter the components accurately, since precise mixing ratio of the two parts leads to reproducible pot lives and curing times and, even more important, vulcanizates whose properties come up to specification. Usually it can be meter by weight or volume in the referenced proportions. The discussed encapsulants are two part mixed products specially designed for PV applications.

Although the high resistance of silicones to environmental conditions and UV light, in the case of the condensation-curing of gel silicones, an incorrect amount of catalyst causes the following problems:

Excess amount:

i. Reduced pot lives (no curing when the amounts added are highly excessive);
ii. Tendency to adhere to contact materials (primer effect);
iii. Significantly increased chemical shrinkage;
iv. Post-curing of the vulcanizates under the effect of air humidity (embrittlement);
v. In the case of highly tear-resistant grades, a significant drop in tear strength after a short time;

Insufficient amount:

i. Delayed crosslinking (in extreme cases, only incomplete curing, if any);
ii. Tendency to adhere to contact materials (adhesion effect);
iii. Soft, limp vulcanizates with low mechanical strength and greatly increased susceptibility to swelling.

With addition-curing silicone encapsulants, the actual effects of incorrect metering of component B may vary, the extent depending on the mixing ratio Base (Part A): Curing agent (Part B) and on which component contains the crosslinking agent and which the platinum catalyst. However, a change in the optimum polymer/crosslinking agent ratio and the catalyst concentration always results.

The consequences are listed below:

i. Longer or shorter pot lives (if the mixing ratio departs greatly from that specified, incomplete curing);
ii. Soft, limp vulcanizates with low mechanical strength and greatly increased susceptibility to swelling;
iii. Post-curing of the vulcanizates (with excess crosslinking agent);
iv. Increased susceptibility to inhibition (with catalyst deficiency).

[1] The unit mPa.s corresponds to 0.001 Pa.s (SI). Dynamic viscosity is also represented by centipoise (cP) that corresponds to 10^{-3} Pa.s.

[2] Thermoplastic Urethane (TPU) is a polymeric encapsulant alternative to E.V.A. It presents the problems

Reactivity

The reactivity is described by the pot life and vulcanizing time. The pot life is the period of time over which the catalyzed mix can still be worked and depends greatly on the temperature. The pot life is reduced by heating the compound and extended by cooling.

Vulcanizing times usually specify only the time for the rubber to cure tack-free, i.e. when it can be handled. The ultimate properties of room-temperature-cured rubber, however, are usually reached only after some days. Vulcanizates that are produced at relatively high temperatures usually continue to crosslink to a greater or lesser extent during the subsequent room-temperature ageing. The ultimate properties of the vulcanizate are reached faster by ageing for several hours at relatively moderate temperatures (100–120 °C), otherwise known as post-curing.

Electrical Properties

The electrical properties of the vulcanizate are largely independent of its consistency, reactivity, mechanical properties and the curing system. Most of the properties of the mix and vulcanizate, however, are additionally determined by the type of curing system.

The dielectric strength is the maximum electric field strength that an insulating material can withstand intrinsically without breaking down or experiencing failure.

Primers – Adhesion promoters

Silicones gels are designed to adhere well to a wide variety of substrates (e.g.PV6010), but some the silicone encapsulant products (e.g. Sylgard 184) and some surfaces require adhesion enhancement to achieve adequate bond strength and accelerate adhesion build-up of silicone elastomers to various substrates. Surface treatments to improve adhesion can range from simple cleaning to more complex etching, and may require the application of reactive silane coupling agents in order to achieve optimal bonding.

3.3.3 Silicone degradation

The exposure of silicones to outdoor weather conditions have shown that these durable materials are tolerant to ultraviolet light or ozone and have been successfully tested in many accelerate aging tests. Dow Corning silicones presents a PV modules in which cell encapsulant withstood 25 years with a satisfactory performance. A module rated at 55 W in 1982 as shown in Figure 3.24a produced 52 W in 2008. The IV data is shown in Figure 3.24b. The I_{sc} measured on the module was essentially the same as the initial measurement and, visually, other than being quite dirty the module looks very good [Ketola *et al.*, 2008].

(a)

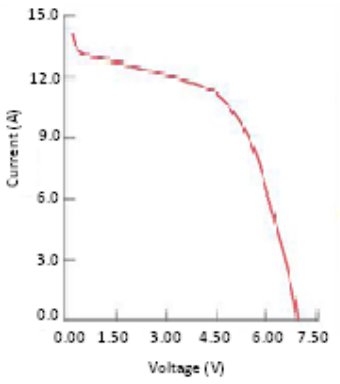

(b)

Figure 3.24 – Module from 1982 and tested in 2008: a) module aspect; b) module I-V curve [adapted from Ketola *et al.*, 2008].

4. Testing different encapsulants for the HSUN PV receiver

This section reports the results of a market survey and describes the experimental procedure in which several tests were carried out to target an encapsulating method for the HSUN PV receiver.

4.1 Available products for encapsulation of PV modules

4.1.1 Polymeric encapsulants – EVA and TPU

Different manufactures were contacted in order to supply samples of EVA and TPU[2] . Table 4.1 presents some of the existing EVA and TPU manufactures and products specification in accordance with the cure type.

Table 4.1- Products and manufactures presentation. A market overview is presented.

Manufacture	Model	Standard Cure	Fast Cure	Ultra Fast Cure
Bridgestone	Evasky	X	X	
Etimex Vistasolar	486.xx		X	
	496.xx		X	
	520.43			X
	517.84 (TPU)		Not required	
Hangzhou First	F806		X	
	F406		X	
Mitsui Fabro	SC52B	X		
	RC02B		X	
Novo Genio	NovoSolar	X	X	
NovoPolymers	NovoVellum CFC3		X	
	NovoVellum UFC4			X
Sanvic	K-series	X		
	F-series		X	
STR	FC280P/UF	X	X	
	15435P/UF		X	X
	25516 (TPU)		Not required	

4.1.2 Backsheets

As previously mentioned, Tedlar from Dupont dominates the backsheet market. The emerging market of backsheets has 10 suppliers, each one of them providing several products. It is possible to find backsheets with two or three layers and with different thicknesses as well (Figure 4.1). With so many variations it is also expected that their properties are very different.

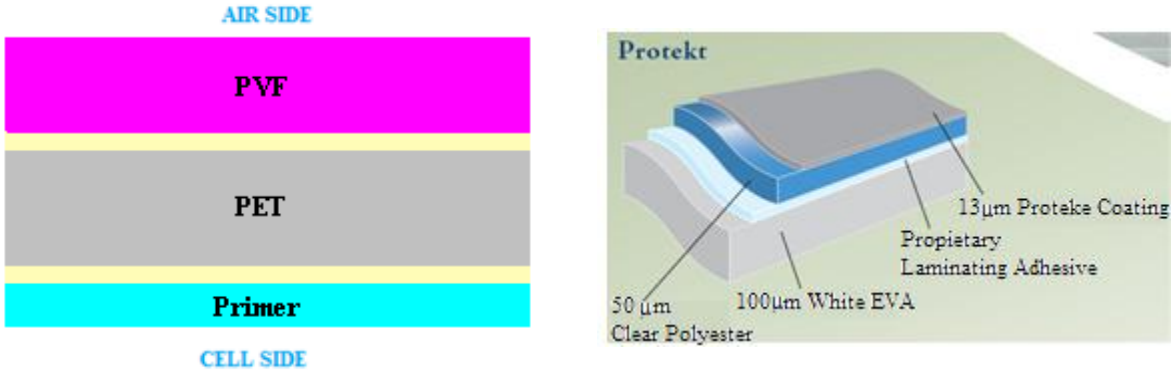

(a) **(b)**

Figure 4.1 – Examples of existing backsheets: a) Double-layer backsheet Icosolar T2823 from Isovolta with Tedlar/PET; b) Triple-layer backsheet with Proteck/EVA/PET from Madico [Madico, 2010].

Backsheet suppliers have been contacted to test their polymeric materials in CPV applications. The feedback from the suppliers Dunmore, Krempel, SFC, MA packaging, Honeywell and Toppan was not obtained, therefore it was not possible to classify their products.


CONFIDENTIAL


CONFIDENTIAL

4.1.3 Silicones

There are four companies that produce silicone encapsulants for PV applications. They are Dow Corning, ACC Silicones Europe, Wacker Silicones and GE Silicones. Table 4.6 shows the main properties of silicone encapsulants from different manufacturers.

4.2 Encapsulation Tests

4.2.1 Preliminary adhesion tests

As mentioned in section 4.1.1, the available material samples for EVA lamination were:

i. Backsheets: BS_1, BS_2,BS_3 and BS_4
ii. EVA encapsulant: ENC_1, ENC_2, ENC_3 and ENC_4

Preliminary adhesion tests were performed after curing at . The lamination process for these preliminary tests did not include the use of vacuum. The temperature and duration of the heating step was not optimized for each particular material.

4.2.2 Lamination tests using EVA

A first set of experiments was performed in order to test the lamination process. Table 4.10 shows the results obtained as well as the problems encountered.


CONFIDENTIAL


CONFIDENTIAL

This module was placed in the first HSUN prototype in the high radiation position (always higher than 15 suns).

[4] See Yellowness Index on Figure 3.14.


CONFIDENTIAL


CONFIDENTIAL

4.2.3 Encapsulation tests using silicone

As discussed in section 3.3, encapsulation using silicone compounds instead of EVA may be of particular relevance for CPV since although more expensive it offers higher optical transmittance and UV resistance.

As previously mentioned in Table 4.6, the available samples are:

i. ENC_6,
ii. ENC_7 and
iii. ENC_{12}[5]

ENC_6 was the encapsulant chosen to start silicone tests (Figure 4.16).

[5] Tests were performed only with ENC_6. The other available samples arrive subsequently to the end of the experimental work.


CONFIDENTIAL


CONFIDENTIAL


CONFIDENTIAL


CONFIDENTIAL

.


CONFIDENTIAL

5. Receiver Heat Transfer Model

5.1 Objectives

The purpose of this chapter is to develop a heat transfer model of the PV receiver for the HSUN in order to assess its cooling requirements and therefore to engineer its assembly.

5.2 Effect of temperature on PV receptor

The operating temperature of a PV receptor is a critical parameter for its efficiency and its ability to withstand long term operation. In this section these effects are briefly reviewed.

5.2.1 Effect of temperature on the solar cell efficiency

The effect of temperature on the performance of a PV module is well known: higher temperatures lead to slightly higher increased short circuit current and significantly lower open circuit voltage. The net effect is the decrease of the efficiency as clearly shown in Figure 5.1.

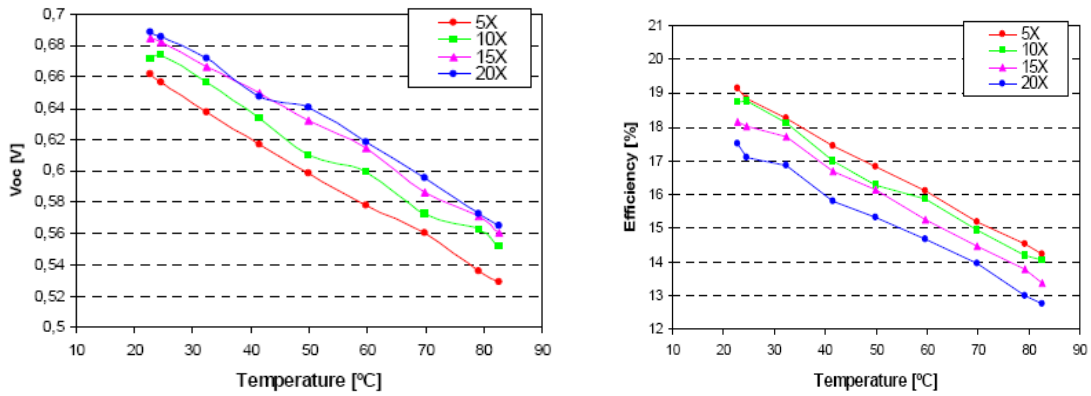

Figure 5.1 – Effects of temperature on V_{OC} and cell efficiency for different concentration values [Morrila *et al.*, 2006].

5.2.2 Effect of temperature on the long term degradation of PV receptor

In polymeric based encapsulants, a higher temperature will result in a decrease of stiffness, leading to distortion or creep in a polymer under an applied load. Section 3.2.3 of this thesis, explains chain scission and crosslinking reactions in polymeric encapsulants, such as EVA. Long term high temperature exposure can also result in changes in mechanical properties of the polymers and the system reliability.

Concerning silicone encapsulants, they are known for high temperature stability and retention properties upon exposure to higher temperatures for during extended periods (Section 3.3.2)

5.3 Heat transfer fundamentals

In order to guarantee the operation of the solar cell within its operating temperature range, one needs to model the heat transfer in the whole PV receptor. In general, heat may be transferred through different mechanisms, like conduction, radiation and convection.

Conduction

The heat transferred through a surface is given by Fourier's law of heat conduction (expression 6).

$$q = -k \, dT/dx \qquad 6$$

Where q, is the heat flow (can be given per unit area W/m^2) and k, thermal conductivity (W/mK).

Across a surface, conduction can be described by expression 7.

$$Q = \frac{kA}{L}(T_1 - T_2) = \frac{T_1 - T_2}{L/kA} \qquad 7$$

Thermal Resistance

Thermal Resistance is the resistance to heat flow created by one surface and it shows a similar behavior to electrical resistance. It depends on the thickness (m), area (m^2) and k (W/mK) (expression 8 and Figure 5.2).

$$R = \frac{L}{kA} \qquad 8$$

Figure 5.2 – Schematic representation of thermal resistance [adapted from Balku, 2010].

Radiative thermal resistance

The radiative heat flow across a surface is described by expression 9.

$$\dot{Q}_{12} = \varepsilon_1 A_1 (\sigma T_1^{\,4} - \sigma T_2^{\,4}) \qquad 9$$

where, ε is the material emissivity (aluminium 0.77), σ the Stephan Boltzmann constant (5.67x10^{-8} W/m^{2}K^4), A the area (m^2), T_1 and T_0 the inside and outside temperatures

Convective heat transfer

Convective heat transfer is the term used to describe heat transfer from a surface to a moving fluid. This flow may be forced, as in the case of a liquid pumped through a pipe, or can be a natural flow, driven by buoyancy forces arising from a density difference, as in the case of a natural-draft cooling tower (expression 10).

$$\dot{Q} = h_c A(\bar{Ts} - Te) \qquad 10$$

where h_c is the convection heat transfer coefficient given by expression 11.

$$\dot{Q}_{conv} = hA_S(T_S - T_\infty) \qquad 11$$

Convective and radiative relation

In a surface exposed to the elements, radiative and convective thermal resistances are parallel systems. In Figure 5.3 the total heat flow is presented.

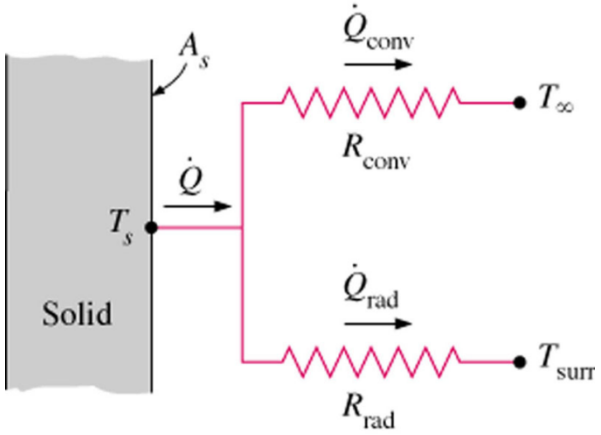

Figure 5.3 – Schematic representation of total heat flow [adapted from

Parallel thermal resistance can be achieved through expression 12.

$$\frac{1}{R_{total}} = \frac{1}{R_{rad}} + \frac{1}{R_{conv}} \qquad 12$$

Passive and active cooling

Figure 5.4 displays some published thermal resistance heat sink values for CPV receptors, including both active and passive cooling.

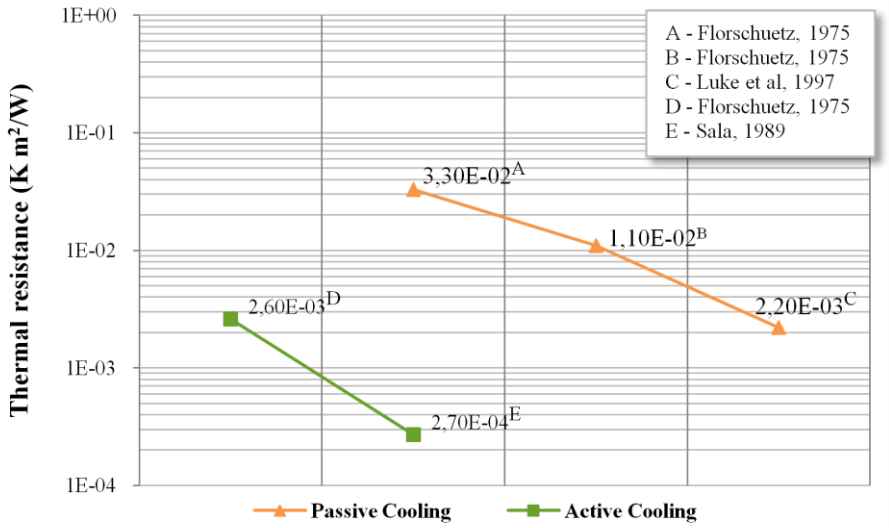

Figure 5.4 - Comparison between different options for passive and active cooling. (A) No extracted surface and calm air. (B) Finned strip, calm air. (C) Finned strip, calm air. (D) Forced air, through multiple passages. (E) Water cooling, plane surface: Turbulent mode (The xx axis is not displayed) [adapted from Royne e*t al.*, 2005].

5.4 Heat transfer model

The heat transfer analysis of the HSUN PV receptor was performed using the HEAT2 software package which is a 2-dimensional transient and steady state heat transfer tool available from Building Physics site (2010).

5.4.1 Irradiation profile

The HSUN PV receptor is exposed to radiation coming from the concentration optics. The normal operating irradiation profile has been developed by [Lopes, 2010] and is shown in Figure 5.5.

For the heat transfer analysis it is essential to consider the effect of misalignments, which may lead to abnormal irradiation profiles, as shown in Figure 5.5 [Lopes, private communication]. It is well known that the performance of the solar cell to an inhomogeneous irradiation profile may be severely detrimental [Luque, 1998]. Here, we shall study its effect on the temperature profile along the solar cell.

When the radiation reaches the PV receptor, it will be reflected, absorbed and transmitted. These interferences are illustrated in Figure 5.6 where incident rays are reflected from the cell (1), air-encapsulant interface (2), encapsulant-backsheet interfaces (3) and the encapsulant interface (4). Furthermore, incident rays are absorbed in the antireflection coating and metal fingers (5), encapsulant (6) and also in the backsheet (7). These interactions depend on the light's incident wavelength and incident angle.

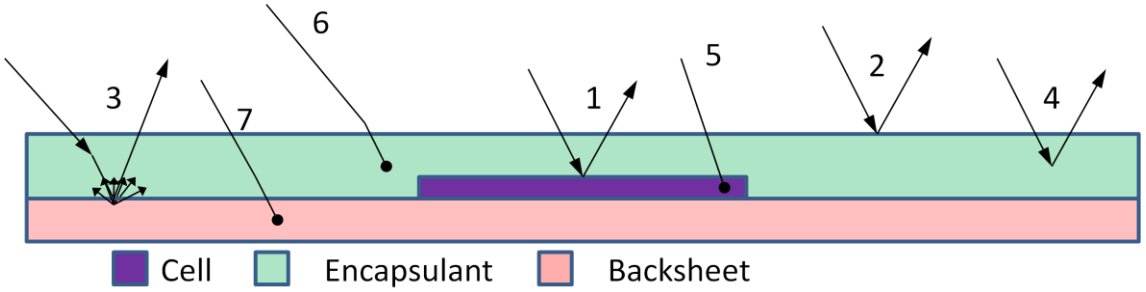

Figure 5.6 - General cross sectional diagram of the thermal model (not to scale) and optical loss mechanisms. (See text for details, adapted from McIntosh *et al.*, 2009).

5.4.2 HSUN PV receptor configuration

The HEAT2 heat transfer tool does not take into account the optical transmissivity of the different materials and therefore, for the purpose of the heat transfer analysis, the models discussed in this chapter are as shown in Figure 5.8, where the top layer (above the solar cell) is not considered. This approximation introduces an error since this top layer is not contributing to lateral heat transfer. However, considering the low thermal conductivity of the EVA and silicone (c.f. Table 5.2), we may neglect this contribution.

Is also possible to note that the optical transmissivity of the EVA and the silicone above the solar cell are very high, respectively 93.3 ± 0.3 and 94.4 ± 0.3 [Kempe, 2008] and therefore, in the model, the radiation that reaches the cell is slightly lower than the designed 15 suns. This small effect was not considered in the model.

Table 5.2 shows the relevant thermal coefficients used for the heat transfer analysis. One should note that the silicon solar cell is considered to be of silicon only, and therefore we are neglecting the

5.4.3 Model geometries

In order to examine the best cooling system for a concentrator it is required the development of a thermal model that will predict heating and electrical output of the cells. The 1-dimensional thermal circuit of the HSUN PV receptor may be described as shown in Figure 5.9 where it is noticeable the equivalent thermal circuits inside the stacks as well as the cooling system and equivalent resistances.

[6] The thermal conductivity values used for Si are the same for standard unprocessed Silicon. Thermal conductivity values were given by manufactures in Private Communications.

All thermal resistances shown in Figure 5.9 may be computed from the data on Table 5.2, except the (radiative and convective) thermal losses at the top and bottom surfaces of the receptor. For the Heat2 analysis, the top surface boundary conditions are defined by the incoming radiation only, and therefore the thermal losses have to be neglected. For typical operating conditions, the temperature of the EVA (or silicone) is kept at 80ºC to avoid material degradation and consequently, using equations 9 and 11, for the bottom surface, the thermal losses are 0.901 Km^2/W for the radiative and 0.2 Km^2/W for convective losses giving an equivalent resistance of 0.164 Km^2/W. This thermal resistance is larger than all the values quoted in Figure 5.10.

A succession of different boundary conditions was analyzed, as shown in Table 5.4. Most of them represent unrealistic heat transfer conditions but were helpful to teach us about the validity of the different approaches.

Models 1 to 3 describe the EVA encapsulated PV receptor. Model 4 describe the Silicone stack.

Since the total power arriving at the cell is 13

$$P_{total} = A_{cell} \times G = Q2_{primary} + Q2_{secondary} \qquad 13$$

the power coming from secondary mirror is

5.4.4 Results

Figure 5.12 shows a typical output from the heat transfer model. However, for our stated purpose, the most relevant output parameters are the maximum solar cell temperature and the temperature variation across the solar cell, since these are the parameters that will determine the PV receptor performance and longevity.

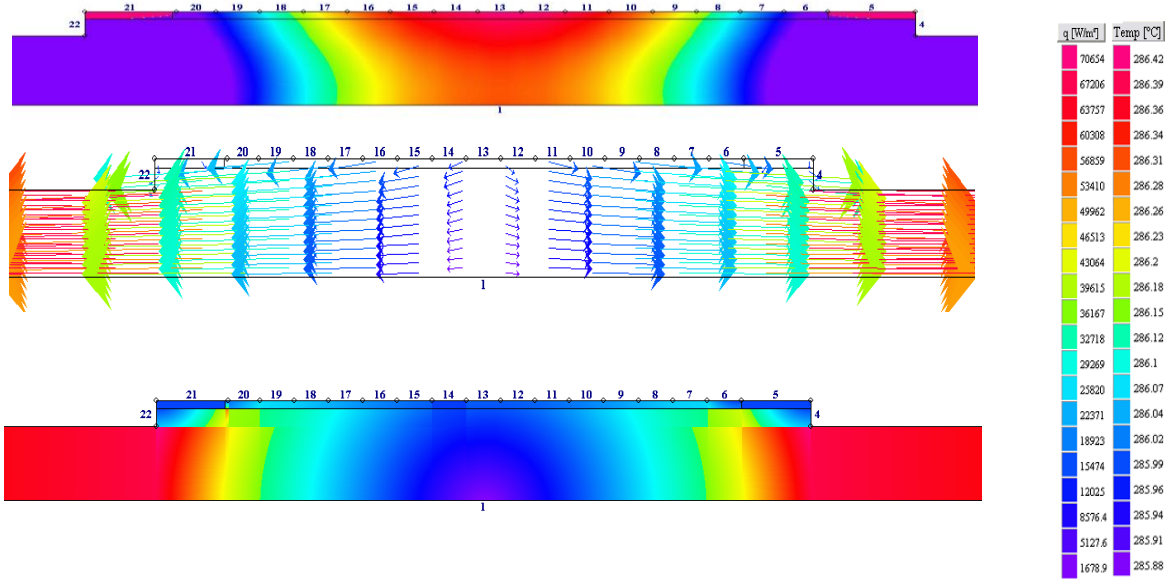

Figure 5.12 – Typical output of the heat transfer model. Model 4 with design incident radiation profile for a . Scales for temperature and heat are presented in the right side. a) Temperature distribution profile. b) Heat flow distribution. c) Heat flow profile.

In order to understand this effect, in Figure 5.14 is shown the comparison between model 3 and model 4 for design incident concentration profile. It is possible observe the temperature distribution across the surfaces. In model 4, the higher temperature is due to an increased resistance in the backsheet. In this case is clear that the heat is not flowing outside.

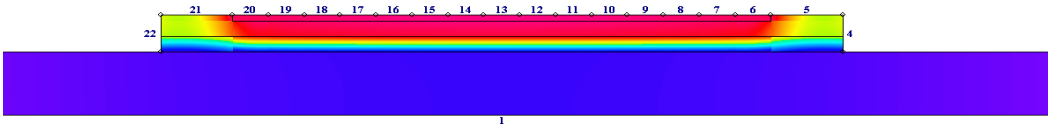

(a)

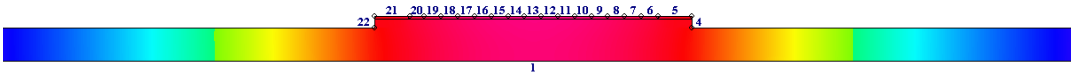

(b)

Figure 5.14 – Comparison between temperature distribution in model 3 and model 4 (a and b, respectively). It is clear that model 4 presents a most homogeneous temperature distribution.

A closer approach to the output of model 3 is shown in Figure 5.15 where the arrows represent heat flow.

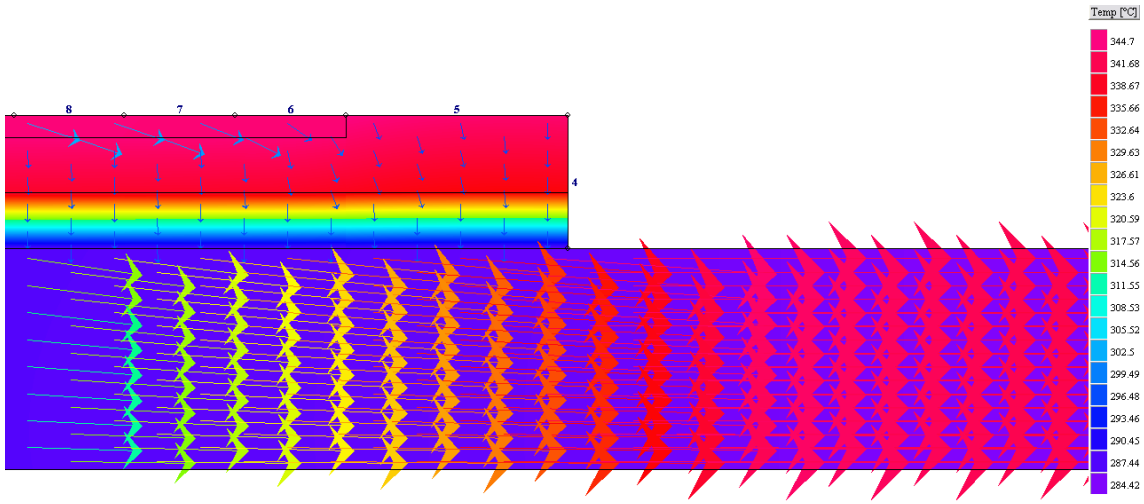

Figure 5.15 – Arrows represent heat flow through model 3. (Design incident concentration profile with a thermal resistivity

Same approach is repeated to model 4 as shown in Figure 5.16. It is possible to observe a slightly heating in silicone neighboring but with lower resistivity (than model 3) due to the better aluminium conduction.

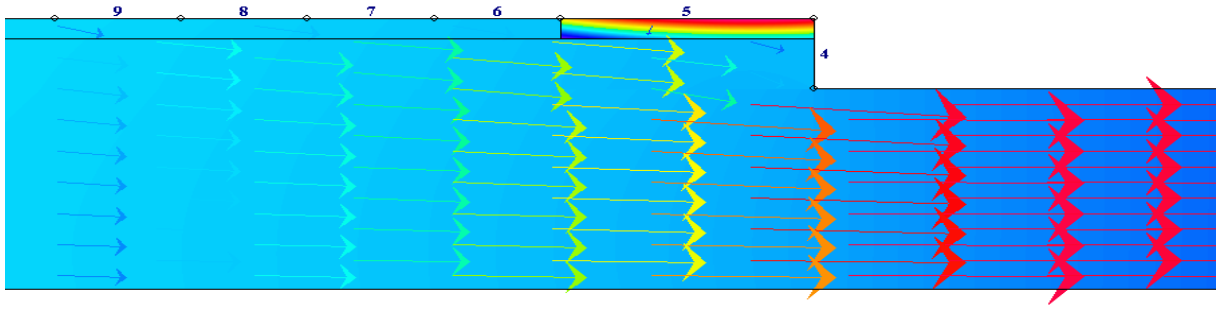

Figure 5.16 - Arrows represent heat flow through model 4. (Design incident concentration profile with a thermal resistivity

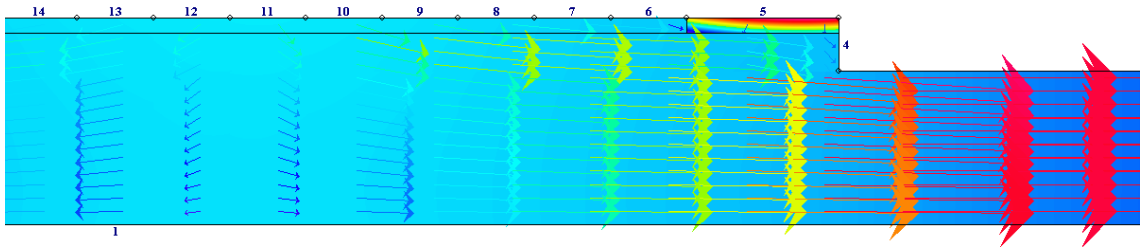

Figure 5.17 – Arrows represent heat flow through model 4. (Worst case Incident Profile with a thermal resistivity of

6. Conclusions

7. Future Plans

8. References

Allen N. S., Edge M., Rodriguez M., Liauw C. M., Fontan E., 2000, Aspects of the thermal oxidation of ethylene vinyl acetate copolymer, Polymer Degradation and Stability, 68, 363-371.

Agroui K., Belghachi A., Collins G., Farenc J., 2007, Quality control of EVA encapsulant in photovoltaic module process and outdoor exposure, Desalination, 209, 1-9.

Amrani, E. A., Mahrane, A., Moussa F.Y., Boukennous Y., 2007, Solar Module Fabrication, International Journal of Photoenergy, doi: 10.1155/2007/27610.

Amonix, 2010, http://mrgreenbiz.wordpress.com/2008/01/03/a-concentrated-power-boost-for-solar-energy/.

Antonini A., Butturi M.A., Benedetto P.D., Milan E., Uderzo D., Zurru P., Parretta A. and Baggio N., 2010, GEN2 *RONDINE*® PV Concentrators, 25th European Photovoltaic Solar Energy Conference on Photovoltaic Energy Conversion, http://www.apollon-eu.org/Assets/0540.pdf.

Bagnall D. M. and Boreland M., 2008, Photovoltaic Technologies, Energy Police, 36, 4390-4396.

Balku S., 2010, http://mechatronics.atilim.edu.tr/courses/mece310/ch9mechatronics.ppt

Baur C., Bett A.W., Dimroth F. and Siefer G., 2007, Triple-junction III-V based concentrator solar cells: Perspectives and challenges, Journal of Solar Energy Engineering, 129, 258-265.

Bosi M. and Pelosi C., 2006, The potential of III-V semiconductors as terrestrial photovoltaic devices, Progress in Photovoltaics: Research and Applications, 15, 51-68.

Bruton T., Mason N., Roberts S., Hartley O.N., Gledhill S., Fernandez J., Russell R., Warta W., Glunz S., Schultz O., Hermle M. and Willeke G., 2003, Towards 20% efficient silicon solar cells manufactured at 60MWp per annum, Proceedings of the Third World Conference on Photovoltaic Energy Conversion, http://www.bp.com/liveassets/bp_internet/solar/bp_solar_spain/STAGING/local_assets/downloads_pdfs/0_999/4pl-e1-01.pdf.

Building Physics, 2010, http://www.buildingphysics.com/index-filer/heat2.htm

Colas, 2005, Silicones in Industrial Applications, Dow Corning Europe, SA, 2-5, http://www.dowcorning.com/content/publishedlit/Silicones_in_Industrial_Applications_Internet_version_080325.pdf.

CPower, 2010, http://www.cpower.it/images/stories/PDF/Rondine_Manual_eng.pdf.

Cuddihy E., Coulbert C., Gupta A. and Liang R., 1986, Electricity from photovoltaic solar cells, Flat-Plate Solar Array Project, Final Report, Volume VII: Module Encapsulation, Jet Propulsion Laboratory Publication 86-31.

Czandema and Pern, 1996, Encapsulation of PV modules using Ethylene vinyl acetate copolymer as a pottant: a critical review, Solar Energy Materials and Solar Cells, 43, 101-181.

Dow Corning Corporation, 1978, Develop silicone Encapsulation Systems for Terrestrial Silicon Solar Arrays, Doe/JPL954995-2.

Dunmore, 2010, http://www.dunmore.com/products/solar-back-sheet.html.

Directive 2002/95/EC of the European Parliament and of the Council of 27 January 2003, Official Journal of the European Union, L 37/19, 13.02.2003, http://eur-lex.europa.eu/LexUriServ/LexUriServ.do?uri=OJ:L:2003:037:0019:0023:en:PDF.

Dupont, 2010, http://www2.dupont.com/Tedlar_PVF_Film/en_US/index.html.

Gebelein C.G., Williams D.J. and Deanin R.D., 1983, Polymers in solar energy utilization, American Chemical Society Symposium Series 220, doi: 10.1021/bk-1983-0220.fw001, http://pubs.acs.org/doi/pdfplus/10.1021/bk-1983-0220.fw001

Green M. A., 2007, Thin-film solar cells: review of materials, technologies and commercial status, Journal of Materials Science: Materials in Electronics, 18, S15–S19.

Guter, W., Schöne J., Philipps, S.P., Steiner M., Siefer G., Wekkeli A., Welser E., Oliva E., Bett A.W., and Dimroth F., 2009, Current-matched triple-junction solar cell reaching 41.1% conversion efficiency under concentrated sunlight, Applied Physics Letters, 94, doi:10.1063/1.3148341.

Heasman K. C., Cole A. , Roberts S. and Bruton T. M., 2007, Laser Grooved Buried Contact Concentrator Cells, NaREC PV Technology Centre, http://concentrating-pv.org/marburg2007/papers/11_Marburg_Paper.pdf

Hering G, 2007, X marks the spot, PHOTON International, April, 123

Holley W. A., 1995, Advanced Development of PV Encapsulants, Semiannual Technical Progress Report, NREL/TP-411-21280, http://www.osti.gov/bridge/product.biblio.jsp?osti_id=258184.

Jorgensen G. J., Terwilliger K. M, DelCueto J. A., Glick S. H., Kempe M. D., Pankow J. W., Pern F. J., McMahon T. J., 2006, Moisture transport, adhesion, and corrosion protection of PV module packaging materials, Solar Energy Materials & Solar Cells, 90, 2739-2775.

Kang Y., Ketola B., McIntosh K., Juen D., Norris A., Tomalia M. K., Shirk C., 2010, The Reliability and Durability of Novel Silicone Materials for Photovoltaic Encapsulation, Dow Corning Corporation, http://www1.eere.energy.gov/solar/pdfs/pvrw2010_poster_kang.pdf.

Kempe M. D., Moricone T., Kilkenny M., 2009, Effects of Cerium Removal From Glass on Photovoltaic Module Performance and Stability, Conference Paper, NREL/CP-520-44936, http://www.nrel.gov/docs/fy09osti/44936.pdf.

Kempe M.D., 2008, Accelerated UV methods and selection criteria for encapsulants of photovoltaic modules, Conference Paper, NREL/CP-520-43300, http://www.nrel.gov/docs/fy08osti/43300.pdf.

Kempe M. D., Jorgensen G. J., Terwilliger K.M., McMahon T. J., Kennedt C. E. and Borek T. T., 2007, Acetic Acid Production and Glass Transition Concerns with Ethylene-Vinyl-Acetate Used in Photovoltaic Devices, Solar Energy Materials and Solar Cells, 91, 315-329.

Kempe M. D., 2006, Modeling of rates of moisture ingress into photovoltaic modules, Solar Energy Materials and Solar Cells, 90, 2720-2738.

Ketola B., McIntosh K. R., Norris A., Tomalia M. K., 2008, Silicones for Photovoltac Encapsulation, 23rd European Photovoltaic Solar Energy Conference, 2-7.

KFW, 2010, http://www.kwfchina.com/en/Product_info.asp?id=12610.

Kho J., 2008, Are thin-film solar efficiency standards unfair?, http://gigaom.com/cleantech/are-thin-film-solar-efficiency-standards-unfair/.

Kurtz S., 2009, Opportunities and Challenges for Development of a Mature Concentrating PV Power Industry, Technical Report, NREL/TP-520-43208, http://www.nrel.gov/pv/pdfs/43208.pdf.

Lopes J. M., 2010, Methods for analysis, optimization and design of optics for photovoltaic concentration, Master Thesis, Instituto Superior Técnico, Universidade Técnica de Lisboa.

Luque A., Sala G. and Luque-Heredia I., 2006, Photovoltaic Concentration at the Onset of its Commercial Deployment, Progress in Photovoltaics: Research and Applications, 14, 413-428.

Luque A. and Hegedus S., 2003, Handbook of Photovoltaic Science and Engineering, Wiley.

Luque A. and Andreev V., 2007, Concentrator Photovoltaics, 1st ed., Springer, chapter 1 and 6.

Luque A., Sala G. and Arboiro J.C., 1998, Electric and thermal model for non-uniformly illuminated concentration cells, Solar Energy Materials and Solar Cells, 51, 269–290.

Madico, 2010, http://www.madicopv.com/products/protekt/.

McIntosh K. R., Cotsell J. N., Cumpston J. S., Norris A. W., Powell N. E. and Ketola B. M., 2009, An Optical Comparison of Silicone and EVA Encapsulants for Conventional Silicon PV Modules: A Ray-Tracing Study, Dow Corning Corporation, http://www.dowcorning.com/content/publishedlit/06-1045.pdf.

Miller D. C., Kempe M. D., Kennedy C. E. and Kurtz S. R., 2009, Analysis of transmitted optical spectrum enabling accelerated testing of CPV designs, Conference Paper, NREL/CP-520-44968, http://www.nrel.gov/docs/fy09osti/44968.pdf .

Morilla M. C., Vivar M., Russel R., Fernández J. M., Sala G., 2006, Developments in the optimization of laser grooved buried contact cells for use in concentration systems, BP, http://www.bp.com/liveassets/bp_internet/solar/bp_solar_spain/STAGING/local_assets/downloads_pdfs/0_999/1DV_3_36.pdf.

Nowlan M., 2007, Development of Automated Production Line Processes for Solar Brigthfield Modules, Subcontract report, NREL/SR-520-43190, http://www.nrel.gov/docs/fy08osti/43190.pdf.

Oerlikon Solar, 2010, http://www.oerlikon.com/ecomaXL/index.php?site=SOLAR_EN_press_releases_detail&udtx_id=7719

Pern J. F.J., 2006, PV Module Encapsulation – Materials, Process, and Reliability, Proceedings of the 16th Workshop on Crystalline Silicon Solar Cells and Modules: Materials and Processes, NREL/BK-520-40423, http://www.nrel.gov/docs/fy06osti/40423.pdf.

Pern, F.J., 1993, Luminescence and absorption characterization of ethylene vinyl acetate encapsulant for PV modules before and after weathering degradation, Polymer Deg. Stability, 41, 125-139.

Pilkington, 2009, Pilkington and the flat glass industry, http://www.pilkington.com/resources/pfgi2009final.pdf.

Poulek V., Libra M. and Persic I., 2008, Bifacial tracking concentrator Traxle 5X, http://www.concentrating-pv.org/darmstadt2009/pdf/papers/20-PoulekLibra-5xTraxleTracker.pdf.

PVCDROM, 2010, http://pvcdrom.pveducation.org/index.html

PVMaT, 2010, Entech, Inc, http://www.nrel.gov/docs/legosti/fy97/21599.pdf.

Reis F., Corregidor V., Brito M. C., Rodrigues R., Wemans J. and Sorasio G., 2009, Power Generation and Energy Yeld Using Doublesun® Photovoltaic Solar Concentration, 24th European Photovoltaic Solar Energy Conference.

Richard D., 2010, Photon International, Solar Power Magazine, August, 236-259.

Rodríguez-Vázquez M., Liauw C. M., Allen N. S., Edge M. and Fontan E., 2006, Polymer Degradation and Stability, 91, 154-164.

Royne A., Dey C.J. and Mills D.R., 2005, Cooling of photovoltaic cells under concentrated illumination: a critical review, Solar Energy Materials & Solar Cells, 86, 451-483.

Saint-Gobain Solar, 2010, http://sg-solar-glass.com/index.php?id=50&L=1.

Sala G., Arboiro, J.C., Luque A., Anton, I et al, 1999, "480 kWpeak EUCLIDES concentrator power plant using parabolic troughs", 2nd World Conference on Photovoltaics Energy Conversion, 1963-1968, http://www.ies-def.upm.es/ies/crating/2WorlConfViena.pdf.

Sanyo, 2010 in http://www.sanyo-solar.eu/en/products/hit-technology/.

SolarSystems, 2010, http://www.solarsystems.com.au/the_technology.html.

Specialized Technology Resources[A], Inc, 2010, Photocap, Solar cell encapsulants, Technical Manual, http://www.strsolar.com/en-us/resources/Documents/photocap_technical_manual_rev2.pdf

Specialized Technology Resources[B], Inc, 2010, Photocap™ Encapsulant Technology, http://www.lstkorea.kr/pdf/EVA/STR%20Brochure.pdf.

Spinoff, 2002, http://www.sti.nasa.gov/tto/spinoff2002/er_7.html.

Spire Solar, 2010, http://www.spirecorp.com/spire-solar/turnkey-solar-manufacturing-lines/index.php.

Sun Power, 2010 , http://us.sunpowercorp.com/.

Swanson, R. M., 2003, Handbook of Photovoltaic Science and Engineering, John Wiley & Sons, Ltd.

Swanson R., 2000, The promise of Concentrators, Progress in Photovoltaics: Research and Applications, 8, 93-111, http://www.solar20.com/resources/Promise%20of%20concentrators.pdf.

Tripanagnostopoulos Y., Souliotis M., Tselepis S., Dimitriou V. and Makris Th., 2005, Design and performance aspects for low concentration photovoltaics, 20th European Photovoltaic Solar Energy Conference and Exhibition.

Wang U., 2008, Solyndra rolls out tube-shaped thin film, http://www.greentechmedia.com/articles/read/solyndra-rolls-out-tube-shaped-thin-film-1542/.

Wohlgemuth J.H. and Petersen R.C., 1991, Solarex experience with EVA encapsulation, Solar Cells, 30, 383-387.

WS Energia, 2010, http://www.ws-energia.com/np4EN/our_technology.

Yang S., 2010, Characterization and Reliability of Polymeric Components in PV Modules, NREL Reliability Workshop, http://www1.eere.energy.gov/solar/pdfs/pvrw2010_poster_yang.pdf.

Zgonena T., 2010, Safety Concerns with New PV Polymeric Materials, Underwriters Laboratories Inc, http://www1.eere.energy.gov/solar/pdfs/pvrw2010_zgonena.pdf.

ZWS, 2010, http://www.zsw-bw.de/index.php?id=109&L=1.